Machine learning methods detect arm movement impairments in a patient with parieto-occipital lesion using only early kinematic information

Annalisa Bosco — Department of Biomedical and Neuromotor Sciences, University of Bologna, Bologna, Italy; Alma Mater Research Institute For Human-Centered Artificial Intelligence (Alma Human AI), University of Bologna, Bologna, Italy

Caterina Bertini — Department of Psychology, University of Bologna, Bologna, Italy; CsrNC, Centre for Studies and Research in Cognitive Neuroscience, University of Bologna, Bologna, Italy

Matteo Filippini — Department of Biomedical and Neuromotor Sciences, University of Bologna, Bologna, Italy

Caterina Foglino — Department of Biomedical and Neuromotor Sciences, University of Bologna, Bologna, Italy

Patrizia Fattori — Department of Biomedical and Neuromotor Sciences, University of Bologna, Bologna, Italy; Alma Mater Research Institute For Human-Centered Artificial Intelligence (Alma Human AI), University of Bologna, Bologna, Italy

Patients with lesions of the parieto-occipital cortex typically misreach visual targets that they correctly perceive (optic ataxia). Although optic ataxia was described more than 30 years ago, distinguishing this condition from physiological behavior using kinematic data is still far from being an achievement. Here, combining kinematic analysis with machine learning methods, we compared the reaching performance of a patient with bilateral occipitoparietal damage with that of 10 healthy controls. They performed visually guided reaches toward targets located at different depths and directions. Using the horizontal, sagittal, and vertical deviation of the trajectories, we extracted classification accuracy in discriminating the reaching performance of patient from that of controls. Specifically, accurate predictions of the patient's deviations were detected after the 20% of the movement execution in all the spatial positions tested. This classification based on initial trajectory decoding was possible for both directional and depth components of the movement, suggesting the possibility of applying this method to characterize pathological motor behavior in wider frameworks.

Introduction

In our daily life, successful reaching movements in the peripersonal space rely on our ability to correctly plan and execute arm trajectories to targets located in the three-dimensional (3D) space. This capacity depends on the coordinated activity of different areas, some of them located in the posterior parietal cortex (PPC). Indeed, unilateral (Karnath & Perenin, 2005; Perenin & Vighetto, 1988) or bilateral (Karnath & Perenin, 2005; Khan et al., 2005; Pisella et al., 2000, 2004) PPC lesions often cause optic ataxia (OA), typically described as a high-order motor disorder

Citation: Bosco, A., Bertini, C., Filippini, M., Foglino, C., & Fattori, P. (2022). Machine learning methods detect arm movement impairments in a patient with parieto-occipital lesion using only early kinematic information. *Journal of Vision*, *22*(10):3, 1–25, https://doi.org/10.1167/jov.22.10.3.

https://doi.org/10.1167/jov.22.10.3 Received July 27, 2021; published September 7, 2022 ISSN 1534-7362

with impaired visually guided reaching (Perenin & Vighetto, 1988). The sites of the lesion in patients with OA typically involve the parietal occipital junction, the superior parietal lobule (SPL), and areas around the posterior end of the intraparietal sulcus (Karnath & Perenin, 2005; Martin, Karnath, & Himmelbach, 2015). These parietal regions have been shown to contain reach-selective neurons in the monkey (Battaglia-Mayer et al., 2001; Bosco, Breveglieri, Chinellato, Galletti, & Fattori, 2010; Bosco, Breveglieri, Hadjidimitrakis, Galletti, & Fattori, 2016; Bosco, Breveglieri, Reser, Galletti, & Fattori, 2015; Fattori, Gamberini, Kutz, & Galletti, 2001; Fattori, Kutz, Breveglieri, Marzocchi, & Galletti, 2005; Ferraina et al., 1997; Grafton, 2010; Hwang, Hauschild, Wilke, & Andersen, 2014; McGuire & Sabes, 2011; Snyder, Batista, & Andersen, 1997) and in the human (Aflalo et al., 2015; Zhang et al., 2017) brain.

OA is characterized by misreaching toward peripheral (Rossetti, Pisella, & Vighetto, 2003) and central (Buiatti, Skrap, & Shallice, 2013; Buxbaum & Coslett, 1997; Ferrari-Toniolo et al., 2014; Goodale et al., 1994; Jeannerod, Decety, & Michel, 1994; Perenin & Vighetto, 1988) visual targets. This deficit does not appear with reaches to auditory or tactile stimuli (Rossetti et al., 2003), thus suggesting that OA is caused from a specific deficit in coupling vision with action. Most OA studies focused on examining reaching end points and on the trajectory of the transport phase of arm movement. In particular, the literature reported a systematic deviation of both end points and movement trajectories for reaching to peripheral targets (Blangero et al., 2010; Dijkerman et al., 2006; Jackson, Newport, Mort, & Husain, 2005; Khan et al., 2007; Milner, Dijkerman, McIntosh, Rossetti, & Pisella, 2003). In addition, patients with OA show a lack of the ability to change the movement trajectory to avoid possible collision with no-target stimuli (Schindler et al., 2004) as well as a lack of the correction of reaching movements in relation to rapid changes of target location (Blangero et al., 2008; Pisella et al., 2000). Monkey studies have demonstrated the link between PPC to the deficits observed in OA by direct causal evidence (Hwang, Hauschild, Wilke, & Andersen, 2012). Furthermore, in monkeys, the existence of a combined encoding of depth and direction signals was found in some PPC sectors during reaching movement (Bosco et al., 2016; Hadjidimitrakis, Bertozzi, Breveglieri, Bosco, et al., 2014; Hadjidimitrakis, Dal Bo', Breveglieri, Galletti, & Fattori, 2015), whereas other sectors showed segregated processing of these signals (De Vitis et al., 2019; Lacquaniti, Guigon, Bianchi, Ferraina, & Caminiti, 1995). In patients with OA, few studies have investigated encoding of depth and direction in reaching movements (Brain, 1941; Cavina-Pratesi, Ietswaart, Humphreys, Lestou, & Milner, 2010; Danckert, Goldberg, & Broderick, 2009; Holmes & Horrax, 1919). In the work by Danckert et al. (2009) in particular, the authors found that the movements executed by patients with OA along the sagittal axis were more impaired than the movements executed along the horizontal axis, thus corroborating the evidence that reach depth and direction might have a distinct neural control.

However, a kinematic characterization of the entire reaching action in 3D space in patients with PPC damage and OA syndrome is still lacking. Here, we reconstructed the movement trajectory and measured the end point errors in one patient with occipitoparietal lesion that reached toward targets located at different depths and directions in 3D space, and we compared them with those measured in healthy participants. Using a novel decoding approach for these studies, we assessed how well kinematic predictors were able to discriminate whether the movement was performed by the patient or by healthy participants and at which stage during movement unfolding. In the long term, our results could provide a methodology for exploring to which extent the available kinematic information could reliably predict an impaired versus a healthy reaching behavior.

Methods

The study was approved by the Ethical Committee of the University of Bologna and carried out in accordance with the recommendations of the Bioethical Committee of the University of Bologna and with the Declaration of Helsinki. All participants gave written informed consent to participate and were naïve to the purpose of the experiment.

Participants

Ten right-handed, healthy control participants took part in this study (mean age, 21.5 ± 2.0; 9 females and 1 male). They all had normal, or corrected to normal, vision. All participants had no history of musculoskeletal or neurological disorders.

In addition to control participants, patient S.T. was also tested. S.T. is a 19-year-old, right-handed man. At the time of testing session, he was a student with 12 years of education. Six years before testing session, at the age of 13, he suffered from a cardiocirculatory arrest, with a resulting vegetative state owing to severe cerebral anoxia. The most recent magnetic resonance image (MRI; 3 years before testing session) documented the presence of altered signal, plausibly owing to ischemic damage in the occipitoparietal cortex in both hemispheres. The lesion was traced manually on the most recent MRI obtained using T1-weighted template MRI scan from the Montreal Neurological Institute

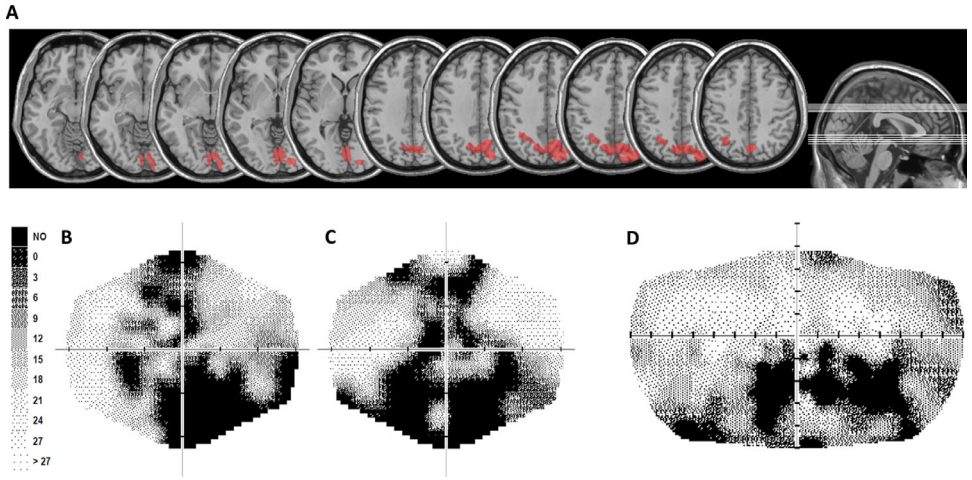

Figure 1. (A) Patient S.T. lesion reconstruction. The image shows patient S.T. lesion projected onto axial slices of the standard MNI brain. In each slice the left hemisphere is on the left side. The levels of the axial slices are marked by white lines on the sagittal view of the brain (right). (B-D) Computerized automated visual perimetry of S.T. Greyscale images for the left (B) and the right (C) eye and for the binocular visual field (D). Axial hash marks denote 10 visual degree increments. Color map reports decibel values corresponding with each point in the gray scale.

provided with the MRIcro software (Rorden & Brett, 2000). Localization of the damaged brain regions was obtained by superimposing the traced lesion reconstruction on the automated anatomical labelling template. Damage in the left hemisphere was located in the superior and inferior parietal lobule, in the angular gyrus and the precuneus, whereas damage in the right hemisphere mainly involved the precuneus (Figure 1A).

Apparatus and stimuli

Participants sat in a dimly illuminated room in front of a 19-inch touchscreen (ELO IntelliTouch 1939L) laid horizontally on a desk located at waist level. The head of participants was supported on a chin rest to minimize movements. Participants sat with the dominant right hand on a board placed adjacent to the screen within a square marked with a tape and detectable by touch (size 12 × 12 cm) placed in front of the participant's chest, as sketched in Figures 2A and 2B.

Green (diameter 0.3 cm) and red (diameter 1.2 cm) dots were presented at different depths and directions with respect to participant's midline. The screen on which stimuli were presented had a visible display size of 37.5 × 30 cm and 15,500 touch points/cm^2 with a resolution of 1152 × 864 pixels and a frame rate of 60 Hz.

Reaching movements were recorded using a motion tracking system (VICON motion capture system) by sampling the position of two markers at a frequency of 100 Hz; markers were attached to the wrist (on the scaphoid bone) and on the nail of the index finger (reaching finger). The marker on the wrist was used to detect the onset and offset of reaching movements. The marker on the tip of the index finger was used for kinematic analysis, because it was the hand portion that made contact with the target (Carey, Hargreaves, & Goodale, 1996).

Behavioral paradigm

Participants performed reaching movements toward the touchscreen using their right hand. As depicted in Figure 2B, there were nine possible locations in which targets could appear: three placed at near distance (18.5 cm from the initial hand position), three at intermediate distance (30 cm from the initial hand position), and three at far distance (41.5 cm from the initial hand position) (as in Bosco, Piserchia, & Fattori, 2017). The targets were arranged in a square of 23 × 23 cm, and were located 11.5 cm one from each other, either on the left or the right side, the central targets were placed along the sagittal midline. All targets were located within a comfortable reaching distance. Although patient S.T. reported visual field defects to the lower parts of the peripheral visual field, he could effortlessly detect all the targets presented in our task. Indeed, stimuli were located in the central part of the visual field, in which S.T. reported no detection impairment. However, he was instructed not to perform any arm movement unless he had a good view of the target.

We tested participants in a visually guided reaching task as shown in Figure 2C. The sequence of visually guided reaching consisted in the presentation of a

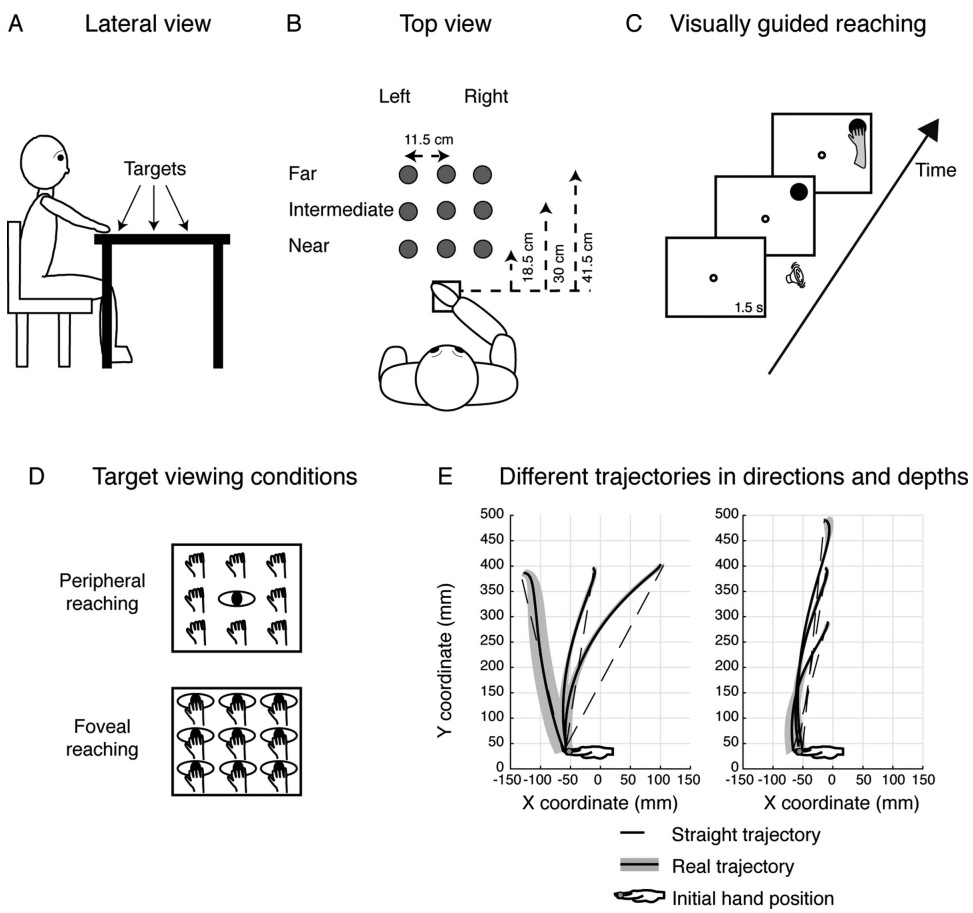

Figure 2. Experimental setup. (A) Lateral view of the target arrangement with respect to the participant's body. (B) Top view of the target arrangement in the peripersonal space. The participants performed reaching movements with their right hand toward one of the nine dots projected on the screen at different depths (near, intermediate, and far) and in different directions (left and right positions). Reaching movements were performed in a dimly lighted room, starting from the initial hand position located next to the body and marked by a squared surface (white square). (C) Time sequence of the visually guided reaching in the peripheral reaching configuration. The small white dot represents the fixation target; the filled black dot represents the reaching target. The fixation target stayed on for 1.5 s and then the reaching target was turned on in one of the nine locations. As soon as the reaching target appeared on the screen, a sound indicated to the participant to reach with his or her right hand the position of the target while maintaining fixation on the fixation target. The fixation target lasted until the participant completed the movement. (D) Top view of the two task configurations. (Top) Peripheral reaching: reaching movements were performed toward one of the nine targets (hands). The spatial position of the target changed trial to trial, but gaze was kept constant at the central position (eye). (Bottom) Foveal reaching: reaching movements were performed toward one of the nine targets. During the task, the participant had to fixate and reach the same target (eye and hand on the panel). (E) Representation of real and straight trajectories in a control participant. (Left) Distribution of the real (shaded traces) and straight (dotted lines) two-dimensional trajectories toward left and right targets (direction dimension). (Right) Distribution of the real (shaded traces) and straight (dotted line) two-dimensional trajectories toward the near, intermediate, and far targets (depth dimension).

fixation target (green dot) that stayed on for 1.5 s. Then, the appearance of reaching target (red dot) and an acoustic signal indicated to participants that they could reach the position of the target maintaining the fixation on the green fixation dot. Both fixation and reaching targets remained illuminated until participants completed the arm movement. Participants were asked to move at a fast but comfortable speed and to be as accurate as possible. We tested two different viewing conditions (see Figure 2D): the peripheral reaching, where the gaze was fixed on the central and intermediate target position and the hand reached toward one of the remaining positions, and the foveal reaching, in which fixation and reaching targets were coincident. Note that the spatial location of the targets to be reached was identical in the two tasks. During the arm movement, fixation was controlled on line by the experimenter. We are aware that this was not a reliable method for

controlling eye movements and represents a limit of the study, but it allowed us to qualitative detect on average 1.2% for each participant and 1.8% for patient S.T. trials where participants did not maintain fixation. Based on this online inspection, all trials without correct fixation were discarded from the analyses.

The task was composed of five blocks with 17 trials each. Within each block, trials of the two viewing conditions were randomized. We used MATLAB (MathWorks, Natick, MA) with the Psychophysics toolbox extension (Brainard, 1997) for stimuli presentation and data analysis.

Data analysis

For data processing and analysis, the velocity profiles of all markers were computed with custom software written in MATLAB. The onset of movement was defined as the time point when wrist velocity was higher than 5 mm/s; the following offset was detected when wrist velocity dropped decreased to less than 5 mm/s. In addition, the experimenter carefully checked for the movement onset that after the threshold of 5 mm/s the wrist velocity increased without interruptions until the peak of velocity. For the movement offset, the first point of wrist velocity remaining below the threshold of 5 mm/s was considered to exclude any adjustment of reaching on the screen.

To study the trajectories of reaching movements and to quantify how participants' motor responses were stereotyped, we calculated the horizontal, sagittal and vertical deviations of each single trajectory with respect to a straight (virtual) trajectory. The virtual straight trajectory was defined as the straight line connecting the starting position of the hand with reaching-target position. This approach has been used by Kasuga, Telgen, Ushiba, Nozaki, and Diedrichsen (2015). Along the horizontal axis we calculated the horizontal trajectory deviation as the difference between the X component of the real trajectory and the X component of the straight trajectory (Figure 2E, left), whereas along the sagittal axis, we calculated the sagittal trajectory deviation considering the difference between the Y component of the real trajectory and the Y component of the straight trajectory (Figure 2E, right). For vertical deviation, we took into account the Z component of the real trajectory, as the straight trajectory had no elevation component. To minimize the interindividual variability observed in movement time and to normalize across participants, horizontal, sagittal, and vertical deviations were separately calculated on 10 time intervals across the entire duration of movement in each participant. The 10 time intervals were calculated for each trial and then averaged across each participant. Then, we plotted the x, y, and z trajectory deviations as a function of the percentage of movement time, resulting in curved lines with negative and positive inflections. Negative values of trajectory deviations correspond with real trajectory on the left, behind, or down with respect to the straight one considering the x, y, or z components, respectively. Positive values of trajectory deviations correspond with real trajectory on the right, in front or up with respect to the straight one according to the x, y, and z trajectory components, respectively. We calculated the time when minimum deviation toward negative values occurred and compared them by a modified version of the independent sample two-tailed t test (Crawford & Garthwaite, 2002; Crawford & Howell, 1998; Danckert, Goldberg, & Broderick, 2009). This analysis allows to test whether an individual's score is significantly different from a control or normative sample and provide a point estimate of the abnormality of the scores (i.e., it estimates the percentage of the population that would obtain a lower score) according to the formula:

$$t = \frac{X_1 - X_2}{S_2\sqrt{(N_2 + 1)/N_2}}$$

where X_1 is the individual's score, X_2 the mean score in the control sample, S_2 the standard deviation of scores in the control sample, and N_2 the number of participants in the control sample. The statistical test follows a t distribution on $N_2 - 1$ d.f. Multiplying the one-tailed probability of t by 100 gives the point estimate of the abnormality of the individual's score in percent.

Decoding from reaching trajectories

To evaluate whether a movement was performed by the patient or a control participant, we adopted a machine learning approach and applied a linear discriminant analysis (LDA). This classification analysis was executed to compare the power of the LDA in recognizing the patient's performance from that of control participants in all targets tested and for both peripheral and foveal conditions. A LDA is a standard classification technique used to allocate a new observation to one of N_G of two or more groups (usually referred to as classes) based on its measured parameters, that in our case are the horizontal, sagittal, and vertical deviations in each temporal division considered (features). The prediction of LDA consists in finding discriminant functions that divide the features space in N_G regions, so that each region spans the range of feature values that most likely characterize a given class. This is done on the basis of a set of previous observations for which the group assignment is known (training dataset), by maximizing the ratio of the

between-groups to within-group variabilities (Marcia, Kent, & Bibby, 1995; Maselli et al., 2017). We divided the whole time interval into 10 equal parts, for each time interval an independent classifier was trained. Features were extracted as follows: deviations were calculated as detailed in the previous section, when the classifier was trained to separate left center and right target positions or near, intermediate and far positions, features always included x, y and z components of the movement. Each time interval comprising 10% of the movement (and corresponding with a single classifier) was further subdivided into three time bins, so each classifier was trained with n consecutive values each corresponding with 3.3% of the movement time. In this way, a temporal information has been provided to the model. The samples thus corresponded to vectors of n elements $\times$ 3 (x, y, and z components), each sample being computed on a possible repetition of the movement (trial). Because the left, middle, right, or three depth levels were considered over six different classifiers, trials corresponding with the same group were considered together, for example, the classifier that considered left deviations was fed with the three positions, namely, near, center, and far from left targets. Also taking together multiple positions, the available trials were few (15 trials), so we used a leave-one-out cross-validation technique to validate our model. Final accuracy results were reported averaging recognition rates over the 15 test set (error bars were 95% bootstrapped confidence intervals). The analysis was proposed to train separate classifiers to resolve a binary classification between patient and single controls (10 combinations), and to compare the power of the LDA in recognizing the patient's performance from that of control participants and in recognizing the performance between healthy participants in all targets tested and for both peripheral and foveal conditions (Figures 11 and 12).

Reaching end point analysis

Movement accuracy and precision were extracted by end points recorded as the x and y coordinates of index finger when it touched the screen and the x and y coordinates of the target locations. The spatial coordinates of the target locations were obtained by recording the X and Y positions of reflective markers placed on the corresponding position of the targets projected on the screen at the end of each experimental session. The two measures were extracted for each control participant and the patient in the peripheral and foveal reaching task. The accuracy was calculated as follows:

$$Accuracy = \sqrt{(x_M - x_{loc})^2 + (y_M - y_{loc})^2}$$

where x_M and y_M are the average end point coordinates and x_{loc} and y_{loc} are the target location coordinates. The precision was calculated as it follows:

$$Precision = mean\left(\sqrt{(x_i - x_M)^2 + (y_i - y_M)^2}\right)$$

where x_i and y_i are the end point coordinates for each trial and x_M and y_M are the average end point coordinates. We statistically compared the accuracy and precision of control participants with those of the patient S.T. using a one-tailed t-test analysis and Bonferroni post hoc tests. The significant level for all analyses was set to 0.05.

Results

Patient S.T. is a young man with bilateral occipitoparietal lesions. MRI reconstructed lesion extent of S.T. revealed damage in the left hemisphere encompassing the superior and inferior parietal lobule, in the angular gyrus and the precuneus, and damage in the right hemisphere, mainly involving the precuneus (Figure 1A). He performed clinical tests reported below in this article and the experimental task described in the Method section.

Clinical tests

A complete neuropsychological examination at the time of testing session showed: attentional deficits (in the subtests "acoustical vigilance," "alertness," "divided attention," and "response flexibility" of the Italian version of the Test of Attentional Performance (Zimmermann & Fimm, 1992; Zoccolotti, Pizzamiglio, Pittau, & Galati, 1994); impairments in executive functions (Tower of London (Culbertson & ZIllmer, 2000), working memory (subtest "Working Memory" of the Italian version of the Test of Attentional Performance; Zimmermann & Fimm, 1992), long-term and short-term spatial memory (Caffarra, Vezzadini, Dieci, Zonato, & Venneri, 2002; Osterrieth, 1944); Corsi-Block tapping test (Spinnler & Tognoni, 1987), and constructive apraxia (Osterrieth, 1944) (Rey-Osterrieth Complex Figure Test (Caffarra et al., 2002). S.T. also showed defective visual exploration abilities (subtest "visual exploration" of the Italian version of the Test of Attentional Performance (Zimmermann & Fimm, 1992; Zoccolotti et al., 1994). S.T.'s performance was within the normal range in verbal memory (short story recall (Novelli et al., 1986); digit span (Orsini et al., 1987), and logical and reasoning abilities (verbal judgments; Spinnler & Tognoni, 1987). The results of neuropsychological

assessment are reported in Table 1. A neurological examination did not show any hemiparesis or motor deficit and did not reveal somatosensory deficit. S.T. reported visual field defects that were mainly confined to the lower peripheral parts of his left and right visual fields, as documented by static perimetry (Medmont M700 automated perimetry apparatus, Melbourne, Australia) (Figures 1B–1D).

At the time of testing, S.T. showed OA as documented by clinical observation. Indeed, while looking at the examiner's nose, S.T. could correctly identify objects located in the periphery, but he could not accurately point to these objects. He also performed a pointing task (Frassinetti, Bonifazi, & Làdavas, 2007), in which he sat at a distance of 57 cm in front of a semicircular apparatus consisting of a vertical transparent plastic support. The transparent plastic support was graduated (in visual degree) and the experimenter, sitting behind the support, could record the final landing position of each pointing movement. The patient's spatial accuracy in pointing was quantified as the difference between the landing position in pointing and the actual target position.

Visual targets (i.e., a pen) were presented randomly in one of three possible positions: in a central position (0°) or to the left or the right of patient's body midline (21°). The patient was instructed to keep his head in a midline position and to fixate on a central point and the fixation was controlled online by the experimenter; he was asked to reach the targets through a pointing movement with the extended index finger, both with the right and the left hand, both in the absence (open loop condition) and in the presence (closed loop condition) of visual feedback of ongoing movement. Specifically, in the open loop condition, a cardboard covered the semicircular apparatus and prevented vision of the arm performing the movement. Ten stimuli per position, in each condition, were presented. In this clinical task, the patient's performance in each condition was compared with the performance of 10 controls (mean age, 43.8 ± 11.4; 6 females) using a modified version of the independent sample two-tailed *t*-test (Crawford & Garthwaite, 2002; Crawford & Howell, 1998; Danckert et al., 2009). The 10 control participants involved in this clinical task were different from those involved in the experimental task described in the next paragraph of this article.

The patient's performance was defective with both hands, both in the open loop and closed loop conditions and irrespective of target position (all Ps < 0.011) with the exception of pointing movements performed with the right hand toward the right target in the closed loop condition ($P = 0.37$) and movements performed with the left hand toward right targets in the closed loop condition ($P = 0.017$) and toward the left and central targets in the open loop condition (all $P > 0.033$). Overall, pointing errors were more pronounced when

	SS/CS/T/ ScS	Cut-off/ES
Attention		
Test of Attentional		
Performance		
Subtest acoustical vigilance		
Reaction times, minutes		
0–5	T = 43	T = 40
5–10	T = 45	T = 40
False reactions, minutes		
0–5	T = 48	T = 40
5–10	T = 36*	T = 40
Subtest alertness (reaction times)		
Without warning	T = 25*	T = 40
With warning	T = 20*	T = 40
Subtest divided attention		
Reaction times	T = 57	T = 40
Omissions	T = 20*	T = 40
Subtest response flexibility		
reaction times	T < 20*	T = 40
False reactions	T = 29*	T = 40
Executive functions		
Tower of London		
Total move score	SS = 64*	SS = 70
Total correct score	SS = 86	SS = 70
Total rule violation	SS < 60*	SS = 70
Total time violation	SS < 60	SS = 70
Total initiation time	SS = 122	SS = 70
Total execution time	SS < 60*	SS = 70
Total problem solving time	SS < 60*	SS = 70
Working memory		
Test of Attentional		
Performance		
Subtest working memory		
Reaction times	T = 54	T = 40
Omissions	T = 20*	T = 40
Memory		
Verbal memory		
Digit span	CS = 3.75	ES = 1
Short story	CS = 8	ES = 1
Visuospatial memory		
Corsi-Block tapping test	CS = 1.75*	ES = 0
Rey-Osterrieth Complex	CS = 0*	ES = 0
Figure Test (memory)		
Logical and reasoning abilities		
Verbal judgments	CS = 42.5	ES = 2
Constructive apraxia		
Rey-Osterrieth Complex	CS = 3*	ES = 0
Figure Test (copy)		
Visual exploration		
Test of Attentional		
Performance		
Subtest visual exploration test		
Target present		
Reaction times	T < 20*	T = 40
Omissions	T = 24*	T = 40

Table 1. Neuropsychological assessment. *Notes.* *A 'Pathological performance. Patient's scores are reported in the left column, while cut-off scores are reported in the right column. CS, correct score; ES, equivalent score; SCS, screening score; SS, standard score; T, T-value. The ES ranges from 0 to 4, with 0 = pathological performance, 1 = borderline performance, and 2–4 normal performance.

	Left Target	Central Target	Right Target
Right hand			
Closed-loop			
Patient S.T.	−6.3*	1.4*	0.5
Controls	0.44	0.05	−0.01
Open loop			
Patient S.T.	8.5*	2*	5.6*
Controls	1.02	−0.02	−0.47
Left hand			
Closed loop			
Patient S.T.	3.8*	1.1*	−1.6
Controls	−0.32	0	−0.59
Open loop			
Patient S.T.	−2.4	1.3	−5.7*
Controls	0.01	0.07	−1.17

Table 2. Pointing performance of patient S.T. and mean pointing performance of controls. *Notes.* Localization errors are expressed in visual degree. Positive and negative values indicate errors toward the right and the left, respectively. Asterisks denote a neuroatypical performance.

pointing was performed with the right hand, in the open loop condition and toward targets located in the left visual space. These results are shown in Table 2.

Analysis of the reaching end points of the experimental task

Patient S.T. and 10 healthy participants performed the visually guided reaching task in 3D space sketched in Figures 2A–2C. They reached visual targets (presented on a horizontal touch screen) at different depths and directions with respect to participant's midline. We tested two viewing conditions: peripheral reaching, where gaze was kept central, uncoupled from the position of reaching target, and foveal reaching, where gaze and reaching target positions were the same (Figure 2D). No gender effect was found on movement time of both peripheral and foveal reaching (one-way analysis of variance; $P = 0.481$ and $P = 0.3728$, respectively).

A typical analysis of reaching end points is shown in Figure 3, where a comparison of the accuracy and precision parameters between the patient and controls was performed by a *t*-test analysis. Figures 3A and 3C show the distribution of average reaching end points corresponding to control participants and patient S.T. in peripheral and foveal reaching, respectively. It is qualitatively evident a higher accuracy and precision of control participants with respect to patient S.T. The statistical results of accuracy and precision analysis are shown in Figures 3B and 3D as color maps. In peripheral reaching, the accuracy was statistically lower when the patient reached the farthest targets (Bonferroni post hoc test, $P < 0.001$), the left-intermediate target (Bonferroni post hoc test, $P < 0.001$), and the nearest central and right targets (Bonferroni post hoc test, $P < 0.05$ and $P < 0.001$, respectively). The precision was significantly lower for all targets tested (Bonferroni post hoc test, $P < 0.001$). In foveal reaching, the accuracy was significantly lower when the patient reached the right targets (Bonferroni post hoc test, $P < 0.001$), the left and right farthest targets (Bonferroni post hoc test, $P < 0.001$) and the nearest central target (Bonferroni post hoc test, $P < 0.001$). The precision was significantly lower for all targets tested except for the nearest central target (Bonferroni post hoc test, $P < 0.001$). In summary, patient S.T. showed a lower accuracy with respect to control participants, giving origin to hypometric and hypermetric misreaches when the targets were located farthest and nearest, respectively. He showed also a decreased precision for all the targets tested.

In addition to abnormalities of reaching end points, we observed differences in performing the trajectory necessary to reach the targets located along the horizontal and sagittal axes. This difference is shown in Figure 4 where the average trajectory of the patient is graphically compared with that of control participants. For all targets tested, abnormal deviations of the patient's trajectory (in red) are visible compared with the controls' ones (in black). From this qualitative observation, we performed a more accurate characterization of the trajectory performance, as described below in this article.

Analysis of trajectory deviation of x, y, and z components for targets along the horizontal axis of the experimental task

Figure 5 shows an analysis of the trajectory deviations, with respect to the straight trajectory, for reaching targets distributed along the horizontal axis in peripheral and foveal conditions (Figures 5, left, and Figure 5, right, respectively). Kinematic data are reported separately for targets located in the left (Figure 5A), middle (Figure 5B), and right (Figure 5C) spaces.

In control participants, the movements toward left targets started with a trajectory that was close to the straight one and then deviated to the left (see Figure 5A, left, black line). At the half of the movement, the trajectory displayed the maximum deviation and then deviation progressively decreased until the end of the movement. The same trajectory evolution was observed in both peripheral and foveal reaching of left targets (compare the black lines in Figures 5A, left, and 5A, right). In the patient, the pattern of trajectory was totally different. For targets located to the left in peripheral condition, S.T. reached the targets following a trajectory that was close to the straight one (Figure 5A, left, red line) and significant deviations toward

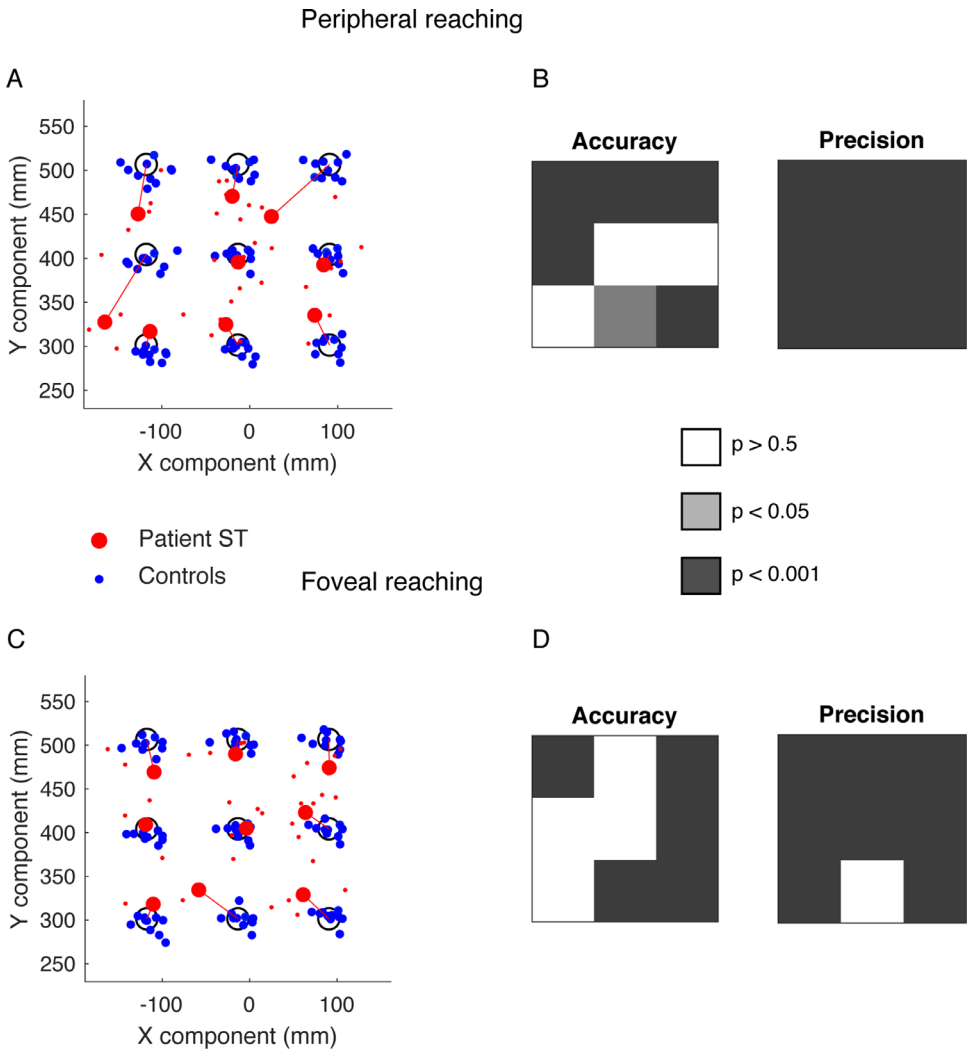

Figure 3. Reaching end points of patient S.T. and control participants. (A) Averaged reaching end points calculated in the peripheral reaching for control participants (blue dots) and patient S.T. (red dots). Red lines represent the patient's end point accuracy (B) *P* values of patient's accuracy (left) and precision (right) in peripheral reaching. (C) Averaged reaching end points calculated in the foveal reaching for control participants (blue dots) and patient S.T. (red). (D) *P* values of patient's accuracy (left) and precision (right) in foveal reaching.

the left (negative values) were observed only in the last 30% of movement execution. In the last 20% of movement, the trajectory was outside the confidence range of the trajectory deviation of the control participants.

In the foveal condition, the trajectory of S.T. toward the left targets was completely different. He showed the maximum leftward (negative) deviation during the first half of movement, with the trajectory being outside the range of control participants deviations from the onset of movement (Figure 5A, right, red line). In the second part of the movement, the trajectory was within the range of control participants and progressively approached the straight line. We calculated the time at which maximum deviation from the straight trajectory occurred. Because the reaching movements toward targets located in the horizontal axis were principally executed along the x component of the trajectory, for left targets, we analyzed the occurrence of maximum negative deviation with respect to the straight trajectory. A significant difference was found in the time where maximum negative deviation occurred in patient and controls in peripheral reaching (controls, 0.31 ± 0.19 s; patient S.T., 0.78 ± 0.1 s; $t = 3{,}076$; $P = 0.013$)., where the deviation occurred later in patient with respect to controls. However, this did not affect the total movement time (controls, 0.73 ± 0.08 s; patient S.T., 0.62 ± 0.07 s; $t = -1.360$; $P = 0.104$). In foveal reaching, no significant difference was found either in the time of maximum negative deviation (controls, 0.27 ± 0.19 s; patient S.T., 0.46 ± 0.36 s; $t = 0.920$; $P = 0.382$) and in the total movement time (controls,

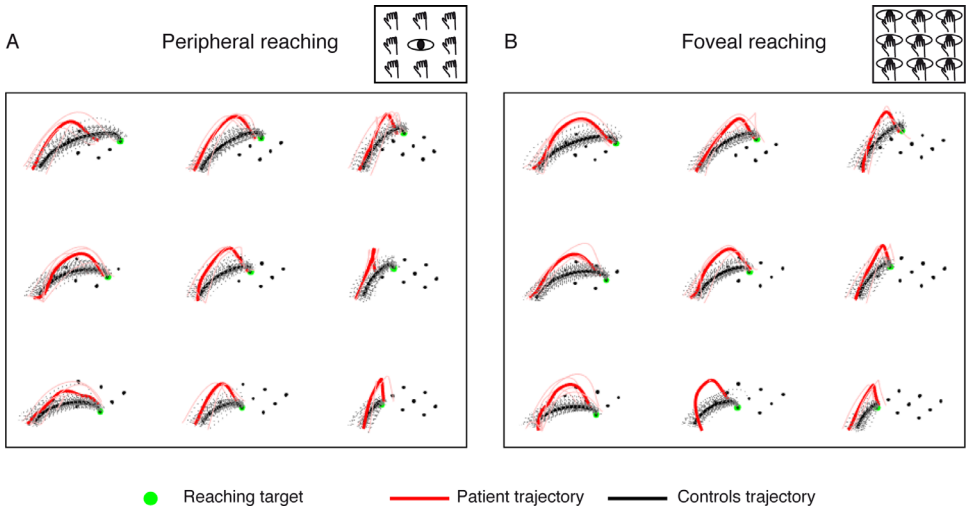

Figure 4. Reaching trajectories of patient S.T. and control participants. (A) Averaged reaching trajectories calculated in the peripheral reaching for control participants (black lines) and patient S.T. (red lines). (B) Averaged reaching trajectories calculated in the foveal reaching for control participants (black lines) and patient S.T. (red lines).

0.72 ± 0.10 s; patient S.T., 0.56 ± 0.09 s; t = −1.480; $P = 0.086$).

For targets located in the middle row, in both peripheral and foveal conditions, control participants presented a negative and a positive peak in trajectory deviations. The first negative peak representing the deviation to the left of the straight trajectory occurred around the 30% of the total movement time (Figures 5B, left, and 5B, right, black lines). The positive peak represented the deviation to the right of the straight trajectory and occurred around the 70% of the movement in both peripheral and foveal condition (Figures 5B, left, and 5B, right, black lines). Patient S.T. started the movement following the same path as control participants, by deviating the arm to the left. However, S.T. was then not able to correct this initial leftward deviation (contrary to the controls) and remained abnormally deviated to the left of straight trajectory for the entire duration of arm movement (Figure 5B, left, red line). This behavior was observed also in the foveal condition (Figure 5B, right). The time where maximum negative deviation that occurred in peripheral (controls, 0.32 ± 0.16 s; patient S.T., 0.40 ± 0.14 s) and foveal conditions (controls, 0.29 ± 0.13 s; patient S.T., 0.52 ± 0.38 s) did not show significant differences (peripheral, t = 0.446; $P = 0.666$, foveal, t = 0.588; $P = 0.571$). No significant differences were found in the total movement time in both peripheral (controls, 0.67 ± 0.16 s; patient S.T., 0.53 ± 0.08 s; t = −0.867; $P = 0.409$) and foveal reaching (controls, 0.67 ± 0.15 s; patient S.T., 0.58 ± 0.19 s; t = −0.551; $P = 0.595$).

For targets located at the right side, in both peripheral and foveal conditions, control participants displayed a pattern of trajectory deviations similar to those observed for reaching toward the middle targets. The first peak, to the left of the straight trajectory, occurred at about the first 30% of movement's duration. The second peak, to the right, occurred at approximately 70% of movement time (Figures 5C, left, and 5C, right, black lines). However, the two negative and positive peaks of trajectory deviations displayed larger amplitudes with respect to those observed in the middle targets. Significant differences between the patient and controls were found in the time where maximum negative deviation occurred in both peripheral (controls, 0.21 ± 0.07 s; patient S.T., 0.55 ± 0.22 s; t = 4.698; $P = 0.001$) and foveal reaching (controls, 0.19 ± 0.07 s; patient S.T., 0.37 ± 0.1 s; t = 2.482; $P = 0.035$). Patient S.T. showed more delayed maximum negative deviations with respect to controls in both reaching conditions. However, no significant differences were found in the total movement time in both peripheral (controls, 0.71 ± 0.11 s; patient S.T., 0.55 ± 0.26 s; t = −1.309; $P = 0.112$) and foveal reaching (controls, 0.71 ± 0.12 s; patient S.T., 0.53 ± 0.08 s; t = −1.388; $P = 0.099$).

These results show that mild, but significant, trajectory deviations were detected also during reaching to left targets in peripheral reaching. However, the worst performance of patient S.T. compared with controls was observed during reaching to right targets, where greater horizontal deviations, distributed across movement execution and delayed maximum negative deviations, were found.

Figure 6 shows the time course of the trajectory deviations for the y component for left (Figure 6A), middle (Figure 6B) and right (Figure 6C) targets in peripheral and foveal reaching. In all target positions, the y deviation of the patient showed less pronounced negative and positive deviations with respect to the

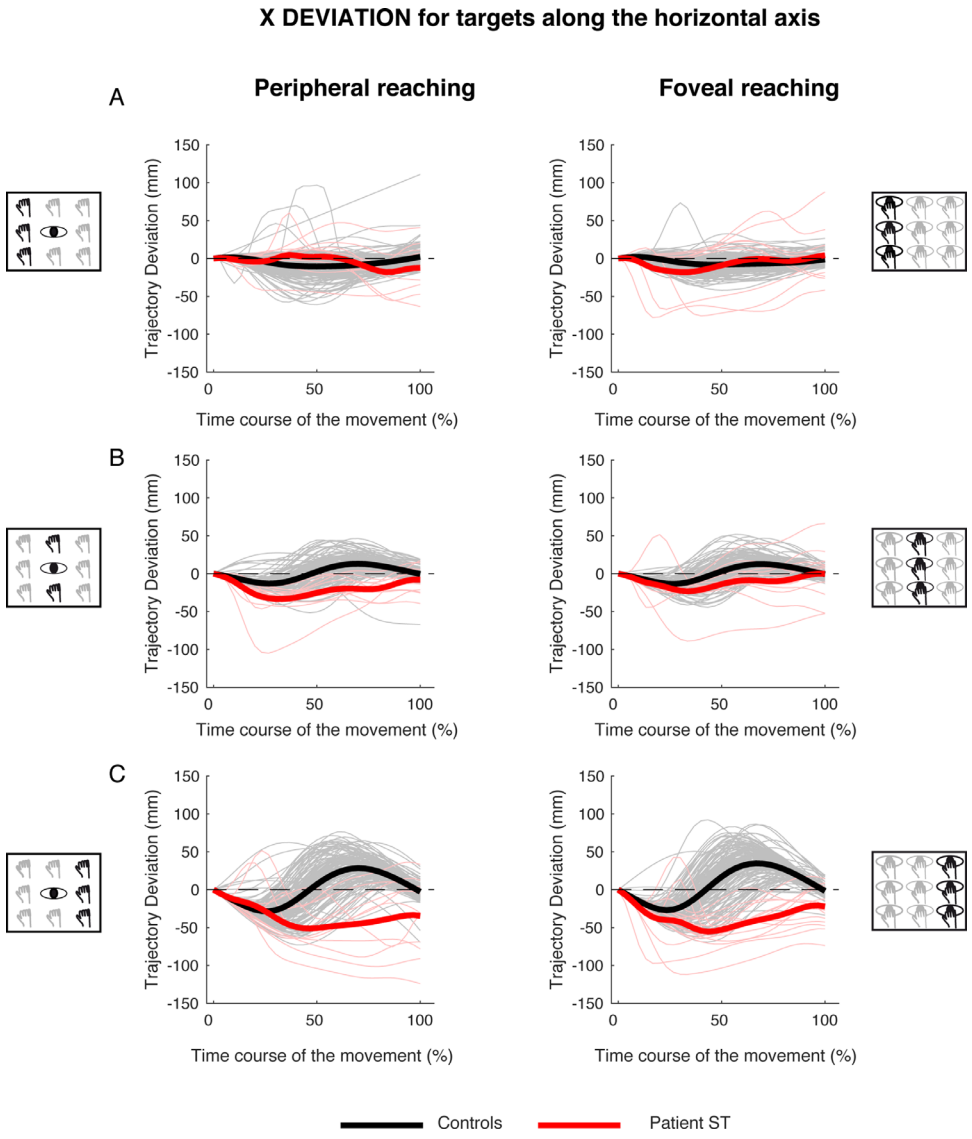

Figure 5. X deviations of reaching trajectory toward targets along the horizontal axis. (A, left) Temporal evolution of the horizontal deviations from the straight trajectory for reaching to left targets in peripheral reaching in patient S.T. (red line) and control participants (black line). Negative values correspond with left deviations, positive values correspond with right deviations. Thin lines represent individual trajectories. (Right) Temporal evolution of the horizontal trajectory deviations for reaching to left targets in foveal reaching. (B, left) Temporal evolution of the horizontal trajectory deviations for reaching to middle targets in peripheral reaching. (Right) Temporal evolution of the horizontal trajectory deviations for reaching to middle targets in foveal reaching. (C, left) Temporal evolution of the horizontal trajectory deviations for reaching to right targets in peripheral reaching. (Right) Temporal evolution of the horizontal trajectory deviations for reaching to right targets in foveal reaching.

controls. In fact, control participants showed first a negative deviation and, during the second stage of the movement, a larger positive one. The averaged positive deviation was 83.2 ± 11.14 mm for peripheral reaching and 91.78 ± 4.99 mm for foveal reaching (see Figures 6A, 6B, and 6C, black lines). In the patient, the averaged positive deviation was 4.77.2 ± 20.6 mm for peripheral reaching and 25.37 ± 2.15 mm for foveal reaching (see Figures 6A, 6B, and 6C, red lines).

Figure 7 shows the time course of the trajectory deviations for the z component for reaching targets distributed along the horizontal axis in peripheral and foveal conditions (Figures 7, left, and Figure 7, right). The kinematic data are reported separately for targets located in the left (Figure 7A), middle (Figure 7B), and right (Figure 7C) spaces. In all target positions tested in the peripheral condition, the control participants showed a single positive peak at the 50%

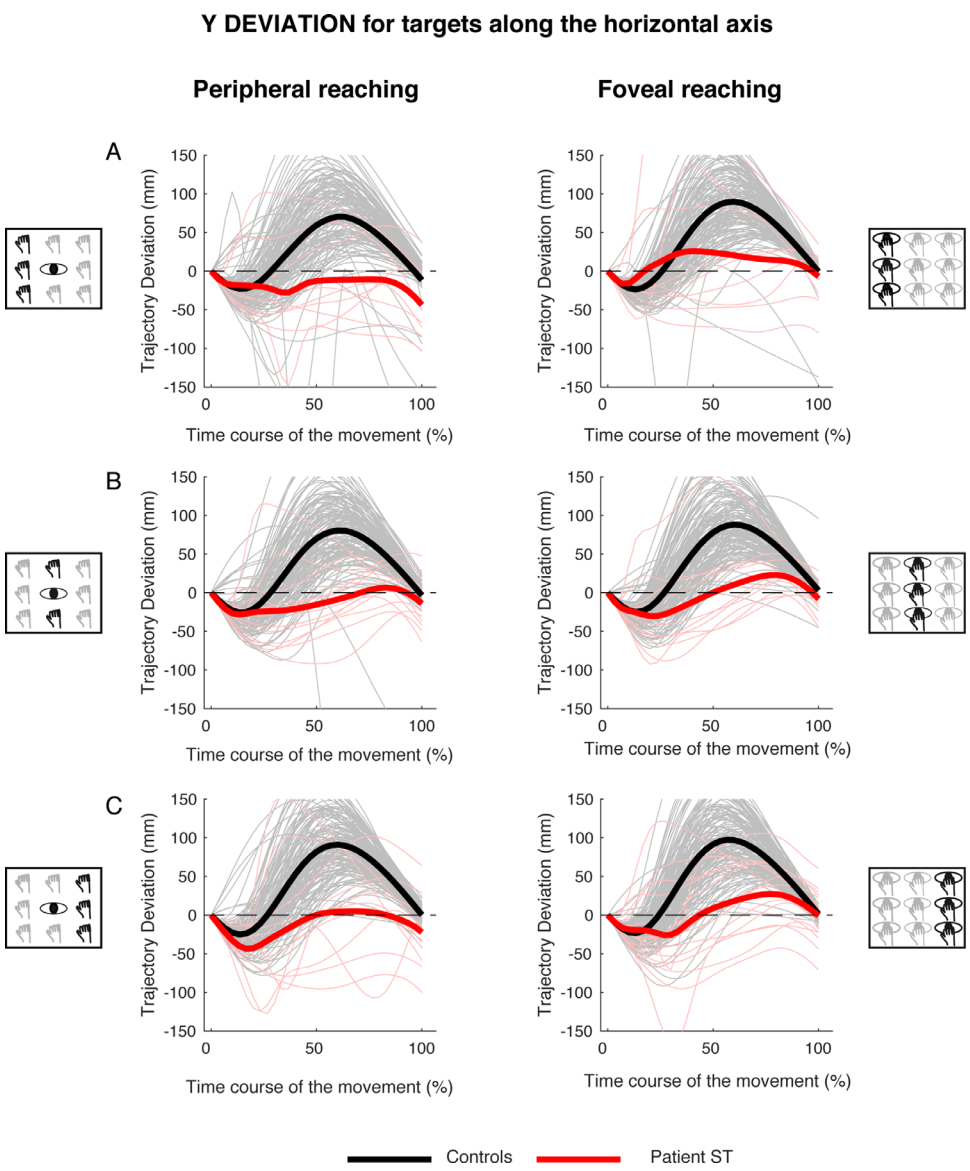

Figure 6. Y deviations of reaching trajectory toward targets along the horizontal axis. (A, left) Temporal evolution of the horizontal deviations from the straight trajectory for reaching to left targets in peripheral reaching in patient S.T. (red line) and control participants (black line). (Right) Temporal evolution of the horizontal trajectory deviations for reaching to left targets in foveal reaching. (B, left) Temporal evolution of the horizontal trajectory deviations for reaching to middle targets in peripheral reaching. (Right) Temporal evolution of the horizontal trajectory deviations for reaching to middle targets in foveal reaching. (C, left) Temporal evolution of the horizontal trajectory deviations for reaching to right targets in peripheral reaching. (Right) Temporal evolution of the horizontal trajectory deviations for reaching to right targets in foveal reaching.

of the movement execution and the averaged deviation was 29.83 ± 17.25 mm. Patient S.T. presented a positive peak more tardive with respect to control participants at the 70% of the movement execution with a larger average deviation equal to 124.84 mm ± 7.51 mm (see Figure 7, left). In foveal condition, the results show similar temporal profiles of positive peaks of deviation between control participants and the patient (50% and 70%, respectively). The average maximum deviation was 30.63 ± 15.91 mm in control participants and 127.97 ± 5.46 mm in the patient (see Figure 7, right).

Analysis of trajectory deviation of x, y, and z components for targets along the sagittal axis of the experimental task

Along the sagittal axis, control participants showed quite consistent trajectory deviations on the x component of the trajectory during reaching movements toward near, intermediate and far targets in both peripheral and foveal conditions. As shown in Figure 8, the control participants showed a negative deviation in the first stage of the movement and a

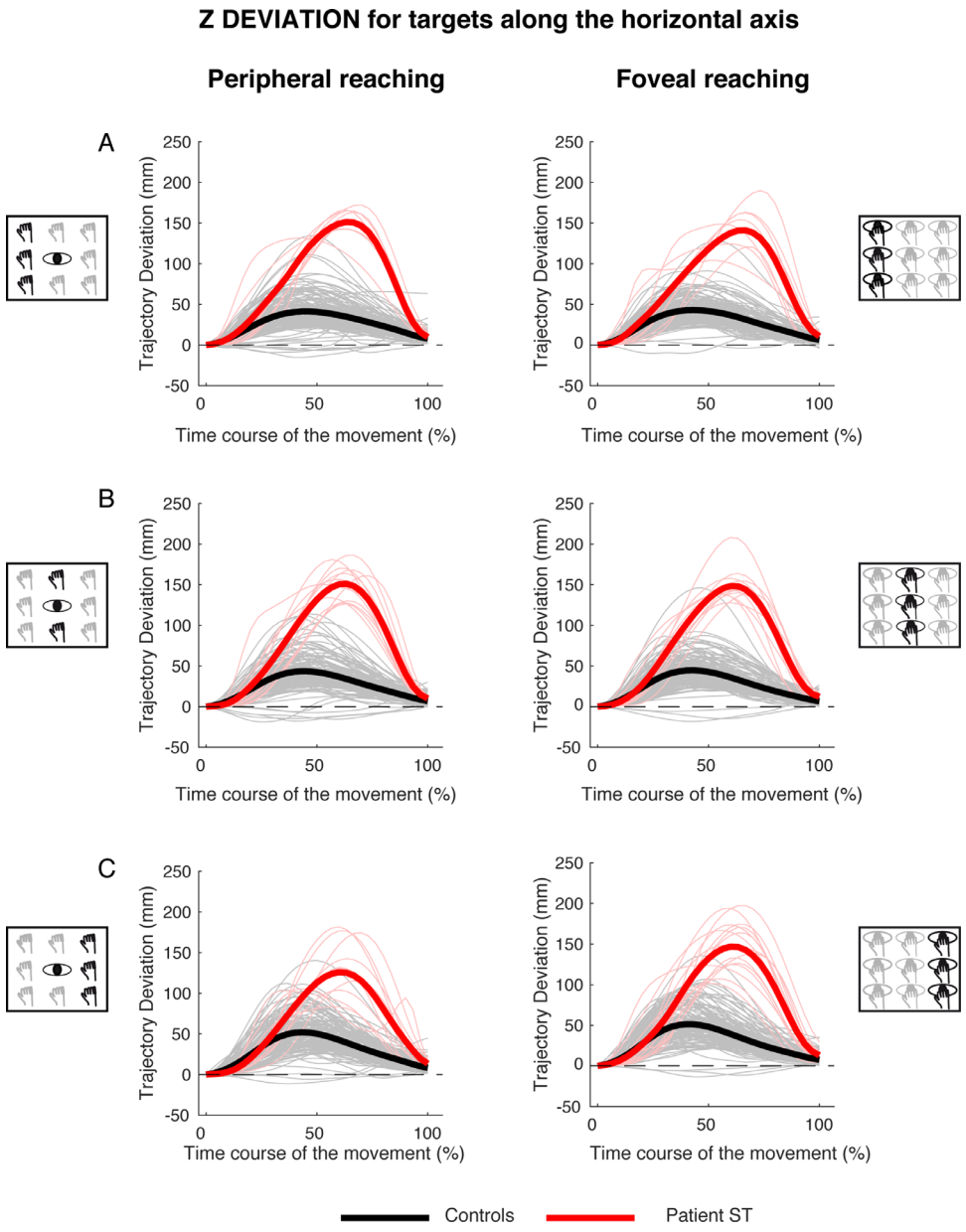

Figure 7. Z deviations of reaching trajectory toward targets along the horizontal axis. (A, left) Temporal evolution of the horizontal deviations from the straight trajectory for reaching to left targets in peripheral reaching in patient S.T. (red line) and control participants (black line). (Right) Temporal evolution of the horizontal trajectory deviations for reaching to left targets in foveal reaching. (B, left) Temporal evolution of the horizontal trajectory deviations for reaching to middle targets in peripheral reaching. (Right) Temporal evolution of the horizontal trajectory deviations for reaching to middle targets in foveal reaching. (C, left) Temporal evolution of the horizontal trajectory deviations for reaching to right targets in peripheral reaching. (Right) Temporal evolution of the horizontal trajectory deviations for reaching to right targets in foveal reaching.

positive deviation in the second stage of the movement for peripheral and foveal reaching (Figures 8A, 8B, and 8C, see black lines). On the contrary, patient S.T. showed only a negative deviation suggesting an inability in correcting the trajectory to appropriately direct the hand toward the final target (Figures 8A, 8B, and 8C, see red lines).

For the y component of the trajectory, control participants showed deviations that gradually increased from near to far targets (Figures 9A, 9B, and 9C, black lines). At the beginning of movement, the hand showed a small hypometric deviation (negative values), which means that it was behind the corresponding point of the straight trajectory. Then, this trajectory deviation

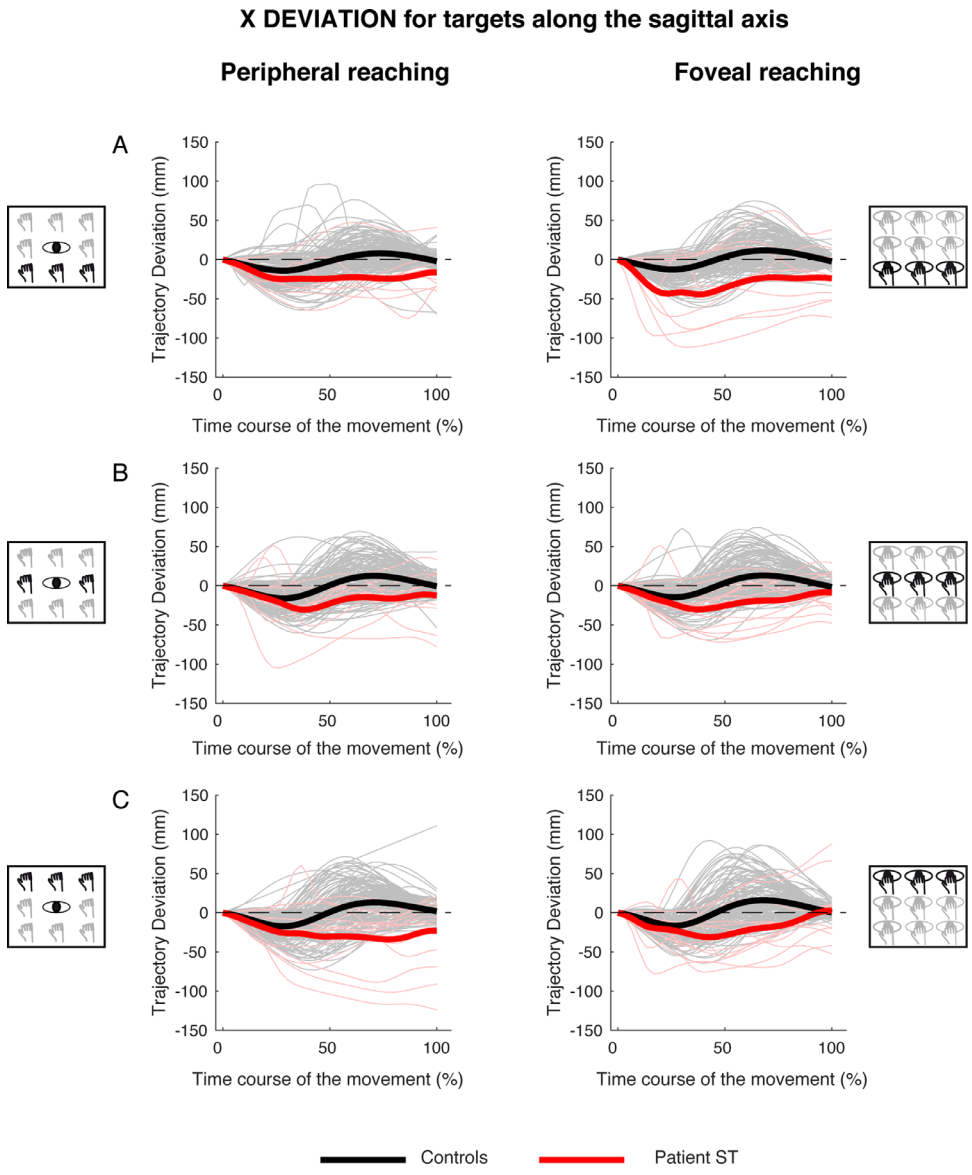

Figure 8. X deviations of reaching trajectory toward targets along the sagittal axis. (A, left) Temporal evolution of the horizontal deviations from the straight trajectory for reaching to near targets in peripheral reaching in patient S.T. (red line) and control participants (black line). (Right) Temporal evolution of the horizontal trajectory deviations for reaching to near targets in foveal reaching. (B, left) Temporal evolution of the horizontal trajectory deviations for reaching to intermediate targets in peripheral reaching. (Right) Temporal evolution of the horizontal trajectory deviations for reaching to intermediate targets in foveal reaching. (C, left) Temporal evolution of the horizontal trajectory deviations for reaching to far targets in peripheral reaching. (Right) Temporal evolution of the horizontal trajectory deviations for reaching to far targets in foveal reaching.

reversed and large hypermetric (positive) values were observed in the remaining 70% of movement (Figure 9, black lines), meaning that the hand was in front of the corresponding point of the straight trajectory. For targets located along the sagittal axis, we calculated the time where maximum deviation toward positive values occurred in patient and controls and then statistically compared them. The patient performed hand movements toward targets at different depths with similar trajectories between the peripheral and foveal reaching (Figure 9, red lines). Patient's trajectories were quite similar to those of control participants in the first 30% of movement, in both peripheral and foveal reaching. However, in the last 70% of movement, trajectories significantly deviated from those of controls, becoming more similar to straight-line trajectories. Notice that, although the control participants showed an increase in deviation for movements toward far targets, the patient showed larger deviations from a straight line trajectory for

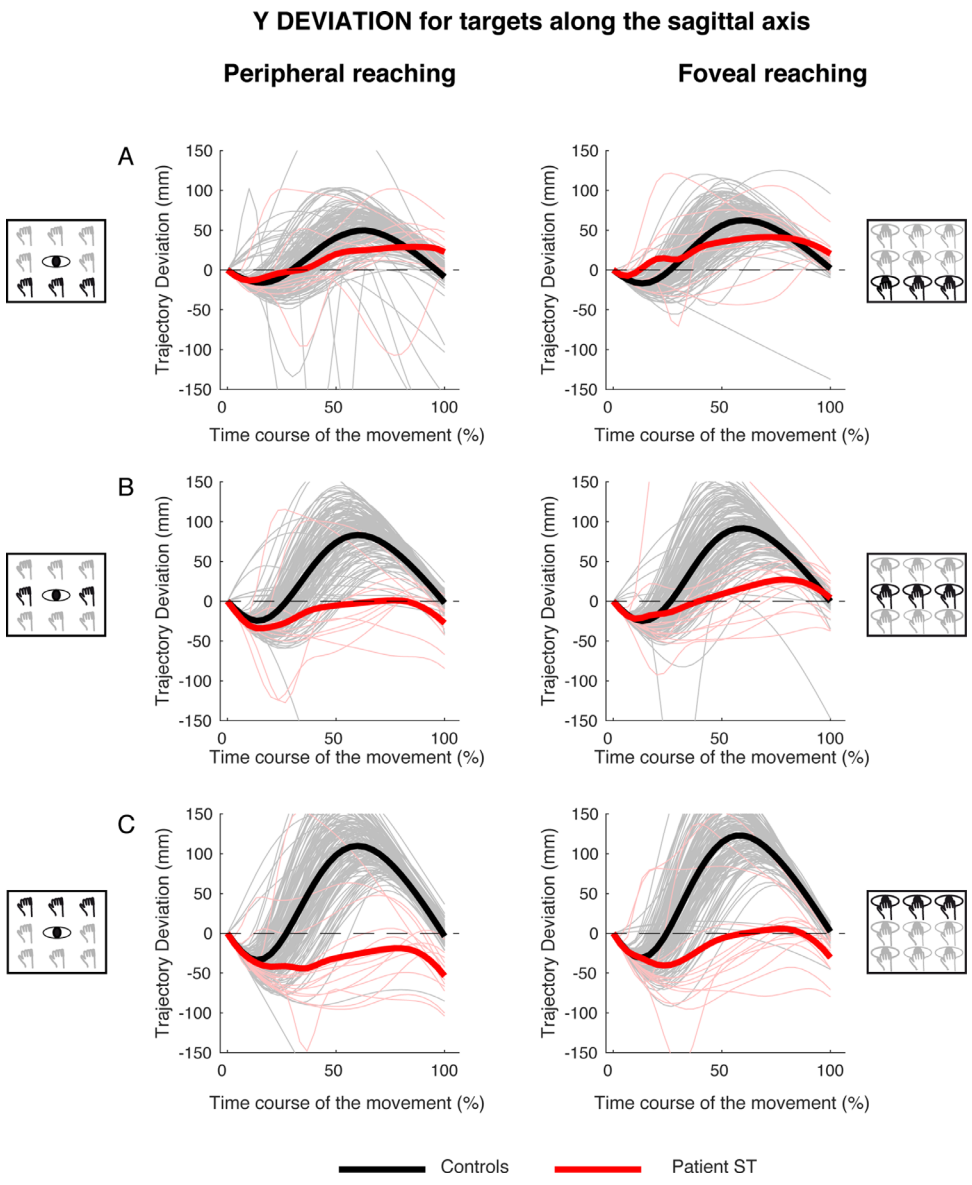

Figure 9. Y deviations of reaching trajectory toward targets along the sagittal axis. (A, left) Temporal evolution of the horizontal deviations from the straight trajectory for reaching to near targets in peripheral reaching in patient S.T. (red line) and control participants (black line). (Right) Temporal evolution of the horizontal trajectory deviations for reaching to near targets in foveal reaching. (B, left) Temporal evolution of the horizontal trajectory deviations for reaching to intermediate targets in peripheral reaching. (Right) Temporal evolution of the horizontal trajectory deviations for reaching to intermediate targets in foveal reaching. (C, left) Temporal evolution of the horizontal trajectory deviations for reaching to far targets in peripheral reaching. (Right) Temporal evolution of the horizontal trajectory deviations for reaching to far targets in foveal reaching.

near targets. No significant differences were found in the time when maximum positive deviation occurred during the movement, both in peripheral (near targets, controls, 0.59 ± 0.1 s; patient S.T., 0.6 ± 0.33 s; t = 0.097; $P = 0.925$; center targets, controls, 0.57 ± 0.09 s; patient S.T., 0.63 ± 0.27 s; t = 0.562; $P = 0.588$; far targets, controls, 0.6 ± 0.08 s; patient S.T., 0.72 ± 0.33 s; t = 1.342; $P = 0.212$) and foveal reaching (near targets: controls, 0.58 ± 0.09 s; patient S.T., 0.59 ± 0.29 s; t = 0.100; $P = 0.923$; center targets, controls, 0.59 ± 0.07 s; patient S.T., 0.72 ± 0.30 s; t = 1.773; $P = 0.110$; far targets, controls, 0.57 ± 0.08 s; patient S.T., 0.68 ± 0.34 s; t = 1.316; $P = 0.221$). However, total movement time was significantly affected only in peripheral reaching for central and far targets (center targets, controls, 0.70 ± 0.09 s; patient S.T., 0.52 ± 0.06 s; t = −2,051; $P = 0.035$; far targets: controls, 0.79 ± 0.09 s; patient S.T., 0.58 ± 0.06 s; t = −2.015; $P = 0.037$).

Figure 10 shows the temporal evolution of the trajectory deviations for the z component for reaching

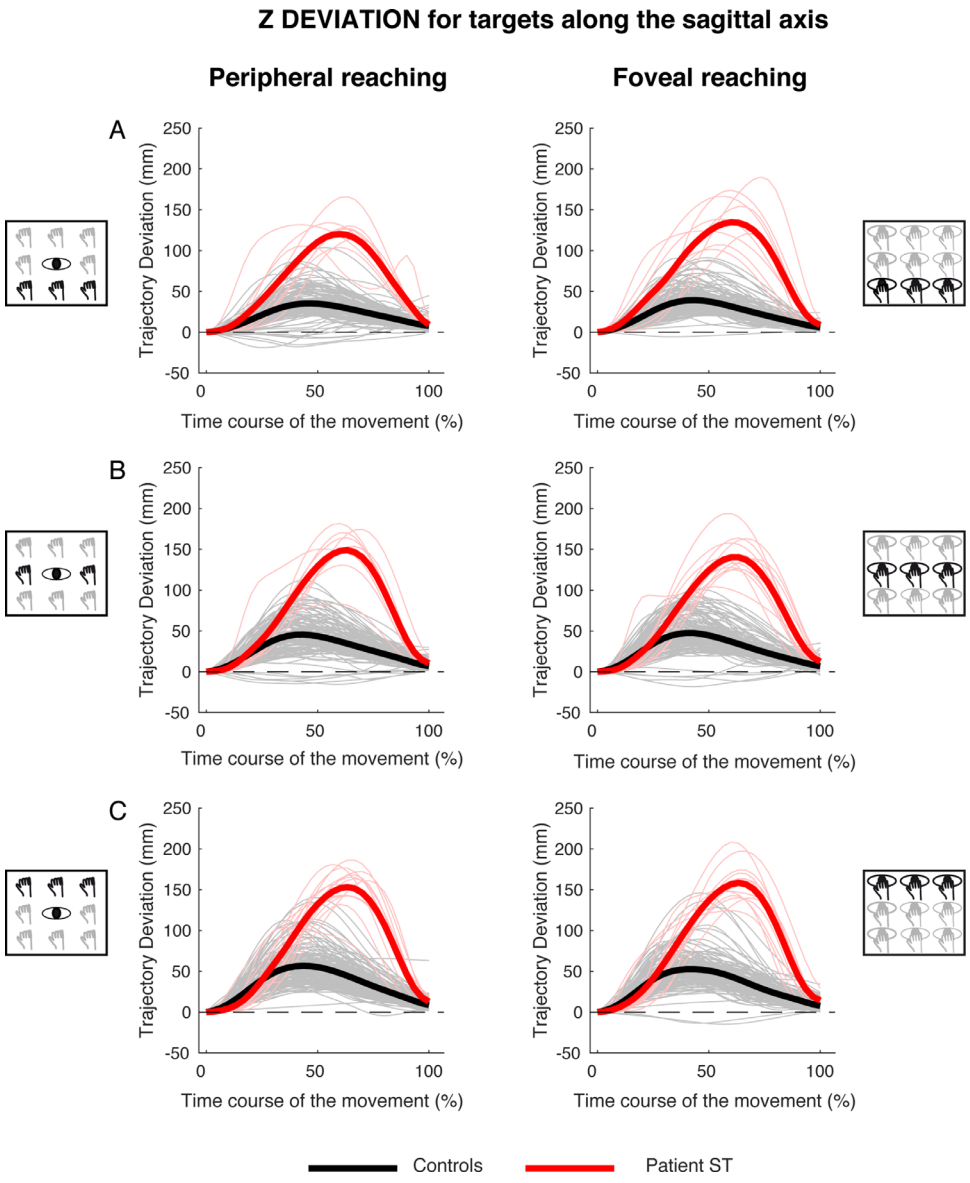

Figure 10. Z deviations of reaching trajectory toward targets along the sagittal axis. (A, left) Temporal evolution of the horizontal deviations from the straight trajectory for reaching to near targets in peripheral reaching in patient S.T. (red line) and control participants (black line). (Right) Temporal evolution of the horizontal trajectory deviations for reaching to near targets in foveal reaching. (B, left) Temporal evolution of the horizontal trajectory deviations for reaching to intermediate targets in peripheral reaching. (Right) Temporal evolution of the horizontal trajectory deviations for reaching to intermediate targets in foveal reaching. (C, left) Temporal evolution of the horizontal trajectory deviations for reaching to far targets in peripheral reaching. (Right) Temporal evolution of the horizontal trajectory deviations for reaching to far targets in foveal reaching.

targets distributed along the sagittal axis in peripheral and foveal conditions (Figure 10, left, and Figure 10, right). In the peripheral condition, similarly at the direction dimension, control participants showed a single positive peak at the 50% of the movement execution and the averaged deviation was 31.05 ± 19.54 mm. Also in this case, patient S.T. presented a positive peak more tardive with respect to control participants at the 70% of the movement execution, with a larger average deviation (116.2 ± 18.14 mm, see Figure 10, left). In foveal condition, the results show similar temporal profiles of positive peaks of deviation in control participants and patient (50% and 70%, respectively). The average maximum deviation was 32.32 ± 17.82 mm in control participants and 121.46 ± 13.55 mm in the patient (see Figure 10, right).

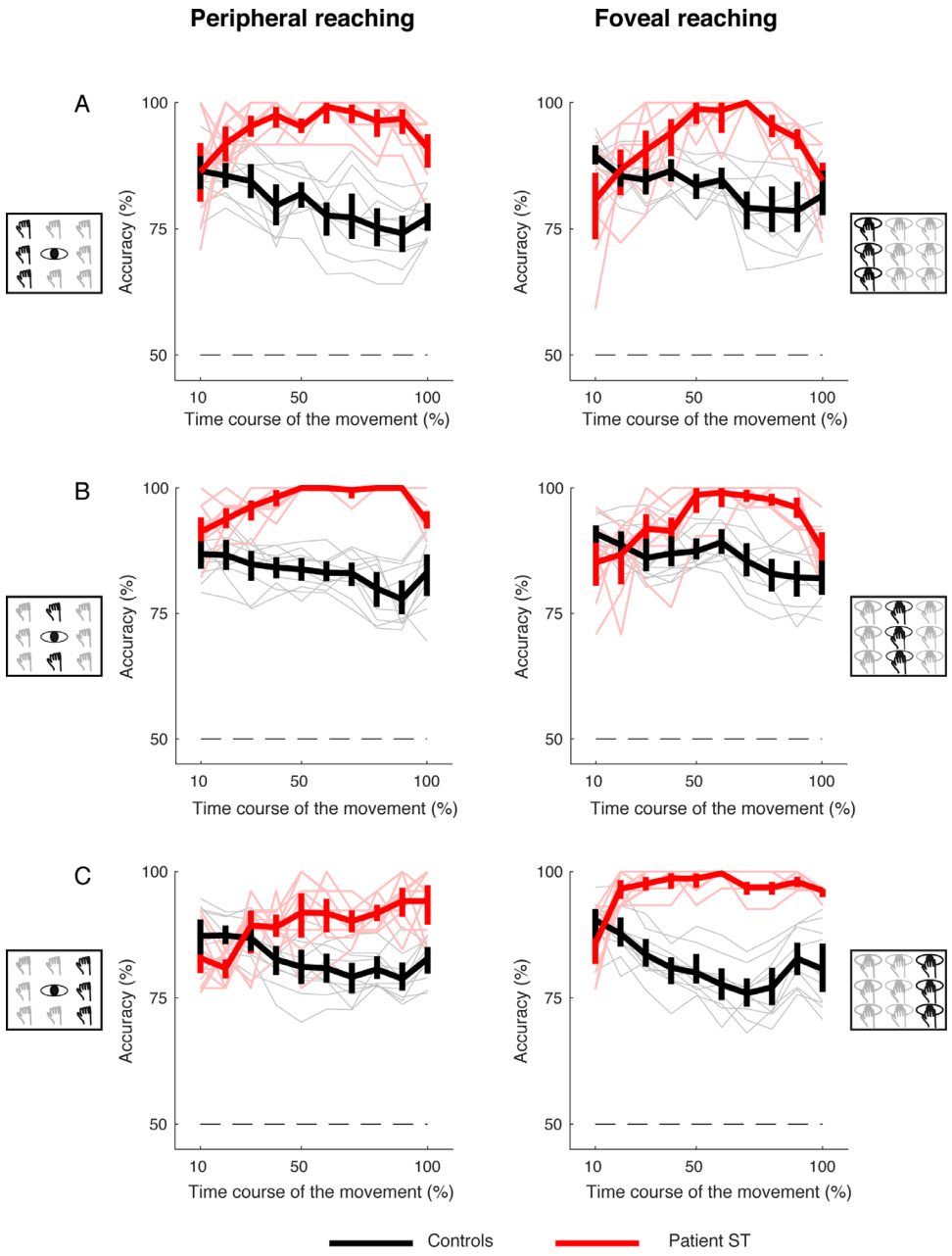

Figure 11. Binary classification analysis aiming to evaluate whether the classifier was able in classifying the patient's performance from each of the controls along the horizontal axis. (A) Average recognition rate of classification accuracy for left targets between patient and controls (red plots) and between controls (black plots). (B) Averaged recognition rate of classification accuracy for middle targets. (C) Averaged recognition rate of classification accuracy for right targets. The thin lines represent individual accuracies. The straight dotted line represents the chance level (50%).

Analysis of the classifier performance

To evaluate whether the performance of the LDA classification analysis, we applied a binary classification analysis that evaluated whether the classifier was more able to discriminate the patient's performance from that of control participants or among controls. Figures 11 and 12 show the average classification accuracy for trajectory deviations across the movement execution for targets located at different directions and depths and in both peripheral and foveal conditions, respectively. We calculated the accuracies through leave-one-out cross-validation and the error bars by 95% bootstrapped confidence intervals. The results show that the classification accuracy was higher in recognizing the patient's performance from that of

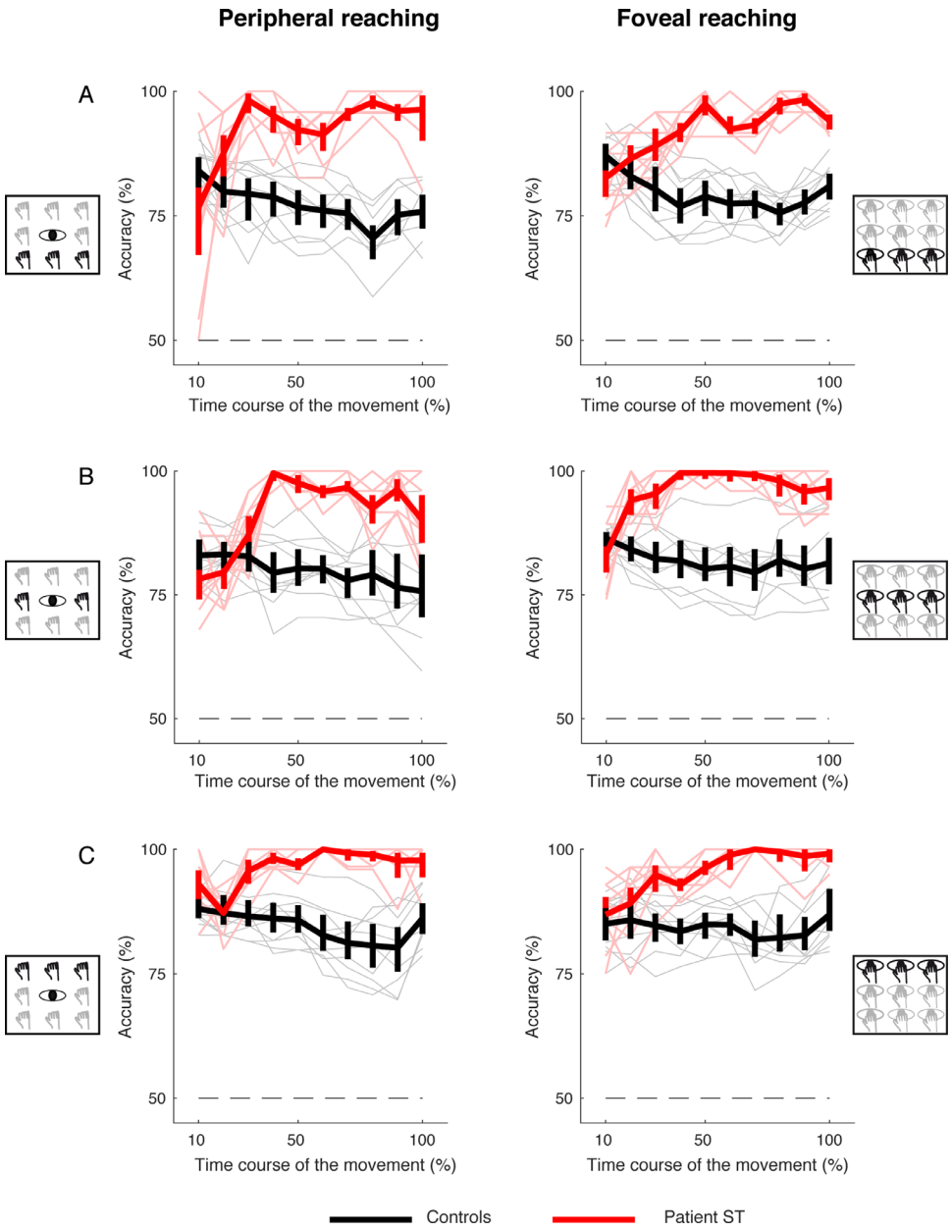

Figure 12. Binary classification analysis aiming to evaluate whether the classifier was able in classifying the patient's performance from each of the controls for targets along the sagittal axis. (A) Average recognition rate of classification accuracy for near targets between patient and controls (red plots) and between controls (black plots). (B) Averaged recognition rate of classification accuracy for intermediate targets. (C) Averaged recognition rate of classification accuracy for far targets. The thin lines represent individual accuracies. The straight dotted line represents the chance level (50%).

control participants when they reached targets in all the positions tested (see the red plots above the black ones in Figures 11 and 12). Furthermore, the ability in the classifier recognition was visible from the 20% of the movement execution, suggesting that, in principle, the method can be generalized as it recognizes better the pathological behavior with respect to the neurotypical one in each condition tested and already at the early stage of the action.

Discussion

The focus of this study was to characterize the kinematics of reaching movements performed toward targets located at different directions and depths in a patient with a bilateral occipitoparietal damage that included parts of SPL, IPS, and precuneus. To do this, we performed a quantification of trajectories by the

adoption of a decoding approach to discriminate, at the individual level, whether reaching movements were performed by the patient or by healthy participants. To our knowledge, this decoding approach has never been applied in studies investigating kinematics in patients with OA.

Because it is well-known that PPC damage can differentially affect movements performed under different viewing conditions (Balint, 1909; McIntosh, Mulroue, & Brockmole, 2010; Rossetti, Pisella, & Vighetto, 2003), we tested here both peripheral and foveal reaching. Although several previous studies have investigated reaching behavior in patients with PPC lesions, and the present findings are in line with these, two aspects of the present study qualitatively deviated from the current literature: the first is the combination of movement trajectory analysis with decoding methods that have not been performed so far, and the second is the joint analysis of reaching errors and trajectories performed toward targets located in the 3D space.

Along the horizontal axis, patient S.T. demonstrated anomalous movement trajectories, significantly more deviated toward the left with respect to control participants for targets located on the right, with peculiar, more delayed negative trajectory deviation. This spatiotemporal impairment, visible both in peripheral and in foveal viewing conditions in the x component of the trajectory, was more evident in the second half of the movement. For targets located on the middle of the reaching space, we also found an anomalous left deviation of the patient S.T. with respect the control participants that was more evident in the peripheral condition after the half of the movement. The abnormal deviations increased from left to middle and then to right targets suggesting a worsening of the reaching performance for the targets included in the most affected visual field of the patient, the right visual field. In line with these findings, during the early stage of the movement, the LDA classifier was able to discriminate the patient's motor performance from that of control participants.

The fact that the patient's abnormal performance is mainly expressed in the second half of the movement, hints at a deficit in the movement correction system that becomes more important in the late stages of movement (Desmurget et al., 1999). This view is in line with the evidence that PPC is responsible for the online correction mechanism of the arm movement (Andersen, Andersen, Hwang, & Hauschild, 2014; Archambault, Ferrari-Toniolo, Caminiti, & Battaglia-Mayer, 2015; Desmurget et al., 1999; Gréa et al., 2002; Pisella et al., 2000; Rossetti et al., 2003). Online correction mechanism is constantly required for the performance of accurate visually guided reaching movements (Goodale, Pelisson, & Prablanc, 1986; Pélisson, Prablanc, Goodale, & Jeannerod, 1986) and requires a fast comparison of target and hand location. This mechanism was demonstrated to be active in reaching movements when rapid changes of target location occurred (Blangero et al., 2008; Pisella et al., 2000). In this situation, patients with OA showed a lack of movement correction. However, the performance of patients with OA improved when the vision of the target and the hand was removed (Jackson, Newport, Mort, & Husain, 2005; Milner, Dijkerman, McIntosh, Rossetti, & Pisella, 2003) because, in these conditions, participants relied on previous knowledge of target location and proprioceptive feedback (Lingnau et al., 2012). All these observations support the view that PPC is involved in online visuomotor control (Desmurget et al., 1999; Gréa et al., 2002; Rossetti et al., 2003). Moreover, movements toward stationary objects (i.e., similar to the movements performed in the present study) have been demonstrated to require slight online modifications in normotypical individuals (Jakobson & Goodale, 1989; Prablanc & Martin, 1992). Given that these modifications produce an increased deceleration time during the second part of the movement, it is reasonable to suppose that the differences found in patient S.T. arm trajectory in the second half of movement execution are correlated with an impairment of such control mechanisms.

Along the sagittal axis, patient S.T. displayed different patterns of trajectory deviations across the target distances tested. The maximum spatiotemporal differences between patient and controls were found for movements performed toward the most distant targets. Moving from near to far space, patient S.T. decreased the trajectory deviation with respect to controls, becoming progressively slower. Specifically, for reaching toward far space, patient's trajectories became more stereotyped compared with those of the controls suggesting a difficulty in relying on the online correction system ascribed to this part of the cortex (Desmurget et al., 1999; Pisella et al., 2000). An additional explanation can be found considering that movements executed along the sagittal plane are more difficult to be executed as they mainly rely on proprioceptive information (van Beers, Sittig, & Denier van der Gon, 1998). In fact, in depth, proprioception is more reliable than vision (Flanders, Tillery, & Soechting, 1992; Monaco et al., 2010; Sainburg, Lateiner, Latash, & Bagesteiro, 2003; van Beers et al., 1998) and the reaching of targets using proprioceptive information is typically more accurate for targets closer to the shoulder (van Beers et al., 1998).

The analysis of trajectory deviations in depth demonstrated differences between peripheral and foveal reaching for near and intermediate targets for the y component of the trajectory. In peripheral reaching and for all target positions, the patient was not able to compensate the trajectory deviation reducing the distance between the deviations of patient S.T. and control participants at the end of movement whereas, in foveal reaching, the patient was able to

reduce this distance that became similar to those of controls (see Figures 9A and 9B, left and right diagrams for comparison). These results reflect the limited impairment of patients with OA in foveal vision (Buxbaum & Coslett, 1997; Jeannerod, Decety, & Michel, 1994; Perenin & Vighetto, 1988) and support strong evidence that described OA as a visuomotor deficit characterized by evident misreaches toward peripherally presented targets.

The majority of case studies on patients with PPC lesions focused on quantifying reaching errors. These studies have demonstrated that patients with PPC lesions, and in particular those presenting the OA deficit, show strong inaccuracies in reaching movements toward targets presented in the contralesional visual field (field effect) and/or using the contralesional hand (hand effect) (Blangero et al., 2008; Khan et al., 2007; Rice et al., 2008; Striemer et al., 2009). Danckert, Goldberg, and Broderick (2009) showed that the damage of SPL including regions of the IPS and parieto-occipital junction led to impaired movements more in the sagittal plane than the horizontal one. Other case studies demonstrated a poor representation of the depth dimension and its perception in patients with bilateral lesions of PPC (Baylis & Baylis, 2001; Holmes & Horrax, 1919; Schaadt, Brandt, Kraft, & Kerkhoff, 2015). The present study confirms that lesions of PPC lead to reaching impairments along both horizontal and sagittal dimensions. Despite different behavioral variables analyzed and the different tasks used to test patients with OA, two studies allow a quantitative comparison with the present study, as they investigated movements executed along horizontal and sagittal dimension (Cavina-Pratesi, Ietswaart, Humphreys, Lestou, & Milner, 2010; Danckert et al., 2009). In these studies, the highest differences between the patients and the control participants were found along the depth dimension, similarly to what we found in the present study (Cavina-Pratesi et al., 2010; Danckert et al., 2009) and in particular for the farthest-contralesional target (Cavina-Pratesi et al., 2010). However, Cavina-Pratesi et al. (2010) found differences only in peripheral viewing conditions, whereas Danckert et al. (2009) found strong impairments in free viewing conditions (foveal conditions), similar to the present results.

There is evidence from monkey studies suggesting the existence of common representation of reaching in depth and direction in single neurons of the SPL (Hadjidimitrakis, Bertozzi, Breveglieri, Bosco, et al., 2014; Hadjidimitrakis, Dal Bo', Breveglieri, Galletti, & Fattori, 2015). These findings from monkeys were in contrast with the general view that depth and direction of reaching targets are processed independently (Crawford, Henriques, & Medendorp, 2011; Flanders, Tillery, & Soechting, 1992). The view of separate pathways for depth and direction is based on several behavioral studies (Bagesteiro, Sarlegna, & Sainburg, 2006; Flanders & Soechting, 1990; Gordon, Ghilardi, Cooper, & Ghez, 1994; Sainburg, Lateiner, Latash, & Bagesteiro, 2003; Van Pelt & Medendorp, 2008; Vindras, Desmurget, & Viviani, 2005), although a neurophysiological support to it is relatively weak (De Vitis et al., 2019; Lacquaniti, Guigon, Bianchi, Ferraina, & Caminiti, 1995). The present work allowed a combined study of direction and depth dimensions, similar to what was done in the monkey (Filippini, Breveglieri, Hadjidimitrakis, Bosco, & Fattori, 2018; Hadjidimitrakis, Bertozzi, Breveglieri, Bosco, et al., 2014; Hadjidimitrakis, Bertozzi, Breveglieri, Galletti, & Fattori, 2017) and, in line with evidence in monkeys, an impairment of reaching in both depth and direction was found. This finding suggests that SPL, in addition to inferior parietal lobule, could contribute to reaching trajectory and movement accuracy performed in 3D space.

This study highlights the possibility to discriminate the performance of a given patient by observing kinematic components of arm movement well in advance with respect to the conclusion of the action. However, without assuming that all patients with OA show a pattern similar to S.T., we predict that the results of the classification analysis can be generalized to other patients on the basis of the extent and location of the lesion that causes the OA and whether the reaching trajectories of the patient display abnormalities with respect to their normal execution that typically presents appropriate curvatures and deviations. Specifically, we would expect a primary deficit in reaching executed toward the 3D space when the OA is associated with lesions that include the SPL, that is known to play a role in the encoding of reaching toward targets located in direction and depth (Bosco, Breveglieri, Hadjidimitrakis, Galletti, & Fattori, 2016; Hadjidimitrakis, Bertozzi, Breveglieri, Bosco, et al., 2014; Hadjidimitrakis, Bertozzi, Breveglieri, Fattori, & Galletti, 2014; Hadjidimitrakis et al., 2017, 2015). In general, and taking into account these considerations, the decoding of patient's reaching behavior by the classifier of the present study could represent a suitable model to examine at which stage of the trajectory, movement inaccuracies develop and this information may be used in clinical applications to evaluate the degree of impairment.

Conclusions

Taken together, these findings suggest that the occipitoparietal lesion results in the impairment of movements toward targets in the 3D space and that these deficits can be decoded well before the movement end. In particular, these impairments affect both movements directed toward targets located along the horizontal axis and movements toward targets located along the sagittal axis in peripheral and foveal reaching conditions. This shows that the PPC is involved in

the encoding of 3D reaching movements as monkey studies demonstrated in the recent literature (Bosco, Breveglieri, Hadjidimitrakis, Galletti, & Fattori, 2016; Hadjidimitrakis, Bertozzi, Breveglieri, Bosco, et al., 2014; Hadjidimitrakis, Bertozzi, Breveglieri, Fattori, & Galletti, 2014; Piserchia et al., 2017). Importantly, the decoding approach applied here to kinematic measures opens a novel perspective in the diagnosis and rehabilitation of visuomotor deficits by analysis of kinematic features of the movement from initial action stages, rather than using the pattern of errors of already accomplished movements.

Keywords: motor control, posterior parietal cortex, target encoding, reaching

Acknowledgments

The authors thank Elisabetta Ladavas for helping in the conceptualization of the study and Kostas Hadjidimitrakis for comments on the article.

Supported by MAIA project, which has received funding from the European Union's Horizon 2020 research and innovation programme under grant agreement No 951910. Ministero dell'Istruzione - Ministero dell'Universita' e della Ricerca awarded to P.F. [PRIN 2017 - Prot. 2017KZNZLN] and to C.B. [PRIN 2017 – Prot. 2017TBA4KS_003].

Author contributions: A.B. designed the research, conducted the experiments, performed the data analysis and wrote the manuscript. C.B. designed the research, performed the analysis and revised the manuscript, M.F. wrote custom software and revised the manuscript. C.F. performed the experiments and data analysis. P.F. designed the research and revised the manuscript.

Data availability statement: The data and codes for this study are available at https://zenodo.org/record/6901261#.Yt-lyi1aYcg.

Commercial relationships: none.
Corresponding author: Annalisa Bosco and Patrizia Fattori.
Email: annalisa.bosco2@unibo.it, patrizia.fattori@unibo.it.
Address: University of Bologna, Piazza di Porta San Donato 2, Bologna 40126, Italy.

References

Aflalo, T., Kellis, S., Klaes, C., Lee, B., Shi, Y., Pejsa, K., . . . Heck, C. (2015). Decoding motor imagery from the posterior parietal cortex of a tetraplegic human. *Science, 348*(6237), 906–910.

Andersen, R. A., Andersen, K. N., Hwang, E. J., & Hauschild, M. (2014). Optic ataxia: From Balint's syndrome to the parietal reach region. *Neuron, 81*(5), 967–983, https://doi.org/10.1016/j.neuron.2014.02.025.

Archambault, P. S., Ferrari-Toniolo, S., Caminiti, R., & Battaglia-Mayer, A. (2015). Visually-guided correction of hand reaching movements: The neurophysiological bases in the cerebral cortex. *Vision Research, 110*, 244–256, https://doi.org/10.1016/j.visres.2014.09.009.

Bagesteiro, L. B., Sarlegna, F. R., & Sainburg, R. L. (2006). Differential influence of vision and proprioception on control of movement distance. *Experimental Brain Research, 171*(3), 358–370, https://doi.org/10.1007/s00221-005-0272-y.

Balint, R. (1909). Seelenlahmung des "schauens" optische Ataxie, raumliche Storung der Aufmerksamkeit. *Monatsschr Psychiatr Neurol, 25*, 51–81. Retrieved from http://ci.nii.ac.jp/naid/10005280654/en/.

Battaglia-Mayer, A., Ferraina, S., Genovesio, A., Marconi, B., Squatrito, S., Molinari, M., . . . Caminiti, R. (2001). Eye-hand coordination during reaching. II. An analysis of the relationships between visuomanual signals in parietal cortex and parieto-frontal association projections. *Cerebral Cortex (New York, N.Y.: 1991), 11*(6), 528–44.

Baylis, G., & Baylis, L. (2001). Visually misguided reaching in Balint's syndrome. *Neuropsychologia, 39*(8), 865–875.

Blangero, A., Gaveau, V., Luauté, J., Rode, G., Salemme, R., Guinard, M., . . . Pisella, L. (2008). A hand and a field effect in on-line motor control in unilateral optic ataxia. *Cortex, 44*(5), 560–568, https://doi.org/10.1016/j.cortex.2007.09.004.

Blangero, A., Ota, H., Rossetti, Y., Fujii, T., Ohtake, H., Tabuchi, M., . . . Pisella, L. (2010). Systematic retinotopic reaching error vectors in unilateral optic ataxia. *Cortex, 46*(1), 77–93, https://doi.org/10.1016/j.cortex.2009.02.015.

Bosco, A., Breveglieri, R., Chinellato, E., Galletti, C., & Fattori, P. (2010). Reaching activity in the medial posterior parietal cortex of monkeys is modulated by visual feedback. *Journal of Neuroscience, 30*(44), 14773–14785, https://doi.org/10.1523/JNEUROSCI.2313-10.2010.

Bosco, A., Breveglieri, R., Hadjidimitrakis, K., Galletti, C., & Fattori, P. (2016). Reference frames for reaching when decoupling eye and target position in depth and direction. *Scientific Reports, 6*(February), 21646, https://doi.org/10.1038/srep21646.

Bosco, A., Breveglieri, R., Reser, D., Galletti, C., & Fattori, P. (2015). Multiple representation of reaching space in the medial posterior parietal

area V6A. *Cerebral Cortex, 25*(6), 1654–1667, https://doi.org/10.1093/cercor/bht420.

Bosco, A., Piserchia, V., & Fattori, P. (2017). Multiple coordinate systems and motor strategies for reaching movements when eye and hand are dissociated in depth and direction. *Frontiers in Human Neuroscience, 11*, 323, https://doi.org/10.3389/fnhum.2017.00323.

Brain, W. R. (1941). Visual disorientation with spatial reference to lesions of the right cerebral hemisphere. *Brain, 64*(4), 244–272, https://doi.org/10.1093/brain/64.4.244.

Brainard, D. H. (1997). The psychophysics toolbox. *Spatial Vision, 10*, 433–436, https://doi.org/10.1163/156856897X00357.

Buiatti, T., Skrap, M., & Shallice, T. (2013). Reaching a moveable visual target: Dissociations in brain tumour patients. *Brain and Cognition, 82*(1), 6–17, https://doi.org/10.1016/j.bandc.2013.02.004.

Buxbaum, L., & Coslett, H. (1997). Subtypes of optic ataxia: Reframing the disconnection account. *Neurocase: The Neural Basis of Cognition, 3*, 159–166.

Caffarra, P., Vezzadini, G., Dieci, F., Zonato, F., & Veneri, A. (2002). Rey-Osterrieth complex figure: normative values in an Italian population sample. *Neurological Sciences, 22*(6), 443–447, https://doi.org/10.1007/s100720200003.

Carey, D. P., Hargreaves, E. L., & Goodale, M. A. (1996). Reaching to ipsilateral or contralateral targets: Within-hemisphere visuomotor processing cannot explain hemispatial differences in motor control. *Experimental Brain Research. Experimentelle Hirnforschung. Experimentation Cerebrale, 112*(3), 496–504, https://doi.org/10.1007/BF00227955.

Cavina-Pratesi, C., Ietswaart, M., Humphreys, G. W., Lestou, V., & Milner, A. D. (2010). Impaired grasping in a patient with optic ataxia: Primary visuomotor deficit or secondary consequence of misreaching? *Neuropsychologia, 48*(1), 226–234, https://doi.org/10.1016/j.neuropsychologia.2009.09.008.

Crawford, J. D., Henriques, D. Y. P., & Medendorp, W. P. (2011). Three-dimensional transformations for goal-directed action. *Annual Review of Neuroscience, 34*(1), 309–31, https://doi.org/10.1146/annurev-neuro-061010-113749.

Crawford, J. R., & Garthwaite, P. H. (2002). Investigation of the single case in neuropsychology: Confidence limits on the abnormality of test scores and test score differences. *Neuropsychologia, 40*(8), 1196–1208, https://doi.org/10.1016/S0028-3932(01)00224-X.

Crawford, J. R., & Howell, D. C. (1998). Comparing an individual's test score against norms derived from small samples. *Clinical Neuropsychologist, 12*(4), 482–486, https://doi.org/10.1076/clin.12.4.482.7241.

Culbertson, W., & Zillmer, E. (2000). Tower of London - DX.

Danckert, J., Goldberg, L., & Broderick, C. (2009). Damage to superior parietal cortex impairs pointing in the sagittal plane. *Experimental Brain Research, 195*(2), 183–191, https://doi.org/10.1007/s00221-009-1766-9.

De Vitis, M., Breveglieri, R., Hadjidimitrakis, K., Vanduffel, W., Galletti, C., & Fattori, P. (2019). The neglected medial part of macaque area PE: Segregated processing of reach depth and direction. *Brain Structure and Function, 224*(7), 2537–2557, https://doi.org/10.1007/s00429-019-01923-8.

Desmurget, M., Epstein, C. M., Turner, R. S., Prablanc, C., Alexander, G. E., & Grafton, S. T. (1999). Role of the posterior parietal cortex in updating reaching movements to a visual target. *Nature Neuroscience, 2*(6), 563–567, https://doi.org/10.1038/9219.

Dijkerman, H. C., McIntosh, R. D., Anema, H. A., de Haan, E. H. F., Kappelle, L. J., & Milner, A. D. (2006). Reaching errors in optic ataxia are linked to eye position rather than head or body position. *Neuropsychologia, 44*(13), 2766–2773, https://doi.org/10.1016/j.neuropsychologia.2005.10.018.

Fattori, P., Gamberini, M., Kutz, D. F., & Galletti, C. (2001). "Arm-reaching" neurons in the parietal area V6A of the macaque monkey. *European Journal of Neuroscience, 13*(12), 2309–2313, https://doi.org/10.1046/j.0953-816x.2001.01618.x.

Fattori, P., Kutz, D. F., Breveglieri, R., Marzocchi, N., & Galletti, C. (2005). Spatial tuning of reaching activity in the medial parieto-occipital cortex (area V6A) of macaque monkey. *European Journal of Neuroscience, 22*(4), 956–972, https://doi.org/10.1111/j.1460-9568.2005.04288.x.

Ferraina, S., Garasto, M. R., Battaglia-Mayer, A., Ferraresi, P., Johnson, P. B., Lacquaniti, F., … Caminiti, R. (1997). Visual control of hand-reaching movement: activity in parietal area 7m. *European Journal of Neuroscience, 9*(5), 1090–1095, https://doi.org/10.1111/j.1460-9568.1997.tb01460.x.

Ferrari-Toniolo, S., Papazachariadis, O., Visco-Comandini, F., Salvati, M., D'Elia, A., Di Berardino, F., … Battaglia-Mayer, A. (2014). A visuomotor disorder in the absence of movement: Does optic ataxia generalize to learned isometric hand action? *Neuropsychologia, 63*, 59–71, https://doi.org/10.1016/j.neuropsychologia.2014.07.029.

Filippini, M., Breveglieri, R., Hadjidimitrakis, K., Bosco, A., & Fattori, P. (2018). Prediction of

reach goals in depth and direction from the parietal cortex. *Cell Reports, 23*(3), 725–732, https://doi.org/10.1016/j.celrep.2018.03.090.

Flanders, M., & Soechting, J. F. (1990). Parcellation of sensorimotor transformations for arm movements. *Journal of Neuroscience, 10*(7), 2420LP–2427LP, https://doi.org/10.1523/JNEUROSCI.10-07-02420.1990.

Flanders, M., Tillery, S. I. H., & Soechting, J. F. (1992). Early stages in a sensorimotor transformation. *Behavioral and Brain Sciences, 15*, 309–320, https://doi.org/10.1017/S0140525X00068813.

Frassinetti, F., Bonifazi, S., & Làdavas, E. (2007). The influence of spatial coordinates in a case of an optic ataxia-like syndrome following cerebellar and thalamic lesion. *Cognitive Neuropsychology, 24*(3), 324–337, https://doi.org/10.1080/02643290701275857.

Goodale, M. A., Meenan, J. P., Bülthoff, H. H., Nicolle, D. A., Murphy, K. J., & Racicot, C. I. (1994). Separate neural pathways for the visual analysis of object shape in perception and prehension. *Current Biology, 4*(7), 604–610, https://doi.org/10.1016/S0960-9822(00)00132-9.

Goodale, M. A., Pelisson, D., & Prablanc, C. (1986). Large adjustments in visually guided reaching do not depend on vision of the hand or perception of target displacement. *Nature, 320*(6064), 748–750, https://doi.org/10.1038/320748a0.

Gordon, J., Ghilardi, M. F., Cooper, S. E., & Ghez, C. (1994). Accuracy of planar reaching movements - II. Systematic extent errors resulting from inertial anisotropy. *Experimental Brain Research, 99*(1), 112–130, https://doi.org/10.1007/BF00241416.

Grafton, S. T. (2010). The cognitive neuroscience of prehension: recent developments. *Experimental Brain Research. Experimentelle Hirnforschung. Experimentation Cerebrale, 204*(4), 475–491, https://doi.org/10.1007/s00221-010-2315-2.

Gréa, H., Pisella, L., Rossetti, Y., Desmurget, M., Tilikete, C., Grafton, S., … Vighetto, A. (2002). A lesion of the posterior parietal cortex disrupts on-line adjustments during aiming movements. *Neuropsychologia, 40*(13), 2471–2480, https://doi.org/10.1016/S0028-3932(02)00009-X.

Hadjidimitrakis, K., Bertozzi, F., Breveglieri, R., Bosco, A., Galletti, C., & Fattori, P. (2014). Common neural substrate for processing depth and direction signals for reaching in the monkey medial posterior parietal cortex. *Cerebral Cortex, 24*(6), 1645–1657, https://doi.org/10.1093/cercor/bht021.

Hadjidimitrakis, K., Bertozzi, F., Breveglieri, R., Fattori, P., & Galletti, C. (2014). Body-centered, mixed, but not hand-centered coding of visual targets in the medial posterior parietal cortex during reaches in 3D space. *Cerebral Cortex, 24*(12), 3209–3220, https://doi.org/10.1093/cercor/bht181.

Hadjidimitrakis, K., Bertozzi, F., Breveglieri, R., Galletti, C., & Fattori, P. (2017). Temporal stability of reference frames in monkey area V6A during a reaching task in 3D space. *Brain Structure and Function, 222*(4), 1959–1970, https://doi.org/10.1007/s00429-016-1319-5.

Hadjidimitrakis, K., Dal Bo', G., Breveglieri, R., Galletti, C., & Fattori, P. (2015). Overlapping representations for reach depth and direction in caudal superior parietal lobule of macaques. *Journal of Neurophysiology, 114*(4), 2340–52, https://doi.org/10.1152/jn.00486.2015.

Holmes, G., & Horrax, G. (1919). Disturbance of spatial orientation and visual attention, with loss of stereoscopic vision. *Archives of Neurology & Psychiatry, 1*(4), 385–407, https://doi.org/10.1001/archneurpsyc.1919.02180040002001.

Hwang, E. J., Hauschild, M., Wilke, M., & Andersen, R. A. (2012). Inactivation of the parietal reach region causes optic ataxia, impairing reaches but not saccades. *Neuron, 76*(5), 1021–1029, https://doi.org/10.1016/j.neuron.2012.10.030.

Hwang, E. J., Hauschild, M., Wilke, M., & Andersen, R. A. (2014). Spatial and temporal eye–hand coordination relies on the parietal reach region. *Journal of Neuroscience, 34*(38), 12884–12892, https://doi.org/10.1523/JNEUROSCI.3719-13.2014.

Jackson, S. R., Newport, R., Mort, D., & Husain, M. (2005). Where the eye looks, the hand follows: Limb-dependent magnetic misreaching in optic ataxia. *Current Biology, 15*(1), 42–46, https://doi.org/10.1016/j.cub.2004.12.063.

Jakobson, L., & Goodale, M. (1989). Trajectories of reaches to prismatically-displaced targets: evidence for "automatic" visuomotor recalibration. *Exp Brain Res, 78*(3), 575–87.

Jeannerod, M., Decety, J., & Michel, F. (1994). Impairment of grasping movements following a bilateral posterior parietal lesion. *Neuropsychologia, 32*(4), 369–380, https://doi.org/10.1016/0028-3932(94)90084-1.

Karnath, H.-O., & Perenin, M.-T. (2005). Cortical control of visually guided reaching: evidence from patients with optic ataxia. *Cerebral Cortex, 15*(10), 1561–1569, https://doi.org/10.1093/cercor/bhi034.

Kasuga, S., Telgen, S., Ushiba, J., Nozaki, D., & Diedrichsen, J. (2015). Learning feedback and feedforward control in a mirror-reversed visual environment. *Journal of Neurophysiology, 114*(4), 2187–2193, https://doi.org/10.1152/jn.00096.2015.

Khan, A. Z., Crawford, J. D., Blohm, G., Urquizar, C., Rossetti, Y., & Pisella, L. (2007). Influence of initial

hand and target position on reach errors in optic ataxic and normal subjects. *Journal of Vision, 7*(5), 8, https://doi.org/10.1167/7.5.8.

Khan, A. Z., Pisella, L., Vighetto, A., Cotton, F., Luauté, J., Boisson, D., . . . Rossetti, Y. (2005). Optic ataxia errors depend on remapped, not viewed, target location. *Nature Neuroscience, 8*(4), 418–420, https://doi.org/10.1038/nn1425.

Lacquaniti, F., Guigon, E., Bianchi, L., Ferraina, S., & Caminiti, R. (1995). Representing spatial information for limb movement: Role of area 5 in the monkey. *Cerebral Cortex, 5*(5), 391–409. Retrieved from http://www.ncbi.nlm.nih.gov/pubmed/8547787.

Lingnau, A., Strnad, L., He, C., Fabbri, S., Han, Z., Bi, Y., . . . Caramazza, A. (2012). Cross-modal plasticity preserves functional specialization in posterior parietal cortex. *Cerebral Cortex, 24*(2), 541–549, https://doi.org/10.1093/cercor/bhs340.

Marcia, K. V., Kent, J. T., & Bibbia, J. N. (1995). Multivariate analysis. In Z. W. Birnbaum, & E. Lukacs (Eds.). San Diego, CA: Academin press.

Martin, J. A., Karnath, H.-O., & Himmelbach, M. (2015). Revisiting the cortical system for peripheral reaching at the parieto-occipital junction. *Cortex, 64*, 363–379, https://doi.org/10.1016/j.cortex.2014.11.012.

Maselli, A., Dhawan, A., Cesqui, B., Russo, M., Lacquaniti, F., & d'Avella, A. (2017). Where are you throwing the ball? I better watch your body, not just your arm!. *Frontiers in Human Neuroscience, 11*, 505. Retrieved from https://www.frontiersin.org/article/10.3389/fnhum.2017.00505.

McGuire, L. M., & Sabes, P. N. (2011). Heterogeneous representations in the superior parietal lobule are common across reaches to visual and proprioceptive targets. *Journal of Neuroscience, 31*(18), 6661–6673, https://doi.org/10.1523/JNEUROSCI.2921-10.2011.

McIntosh, R. D., Mulroue, A., & Brockmole, J. R. (2010). How automatic is the hand's automatic pilot? *Experimental Brain Research, 206*(3), 257–269, https://doi.org/10.1007/s00221-010-2404-2.

Milner, A. D., Dijkerman, H. C., McIntosh, R. D., Rossetti, Y., & Pisella, L. (2003). Delayed reaching and grasping in patients with optic ataxia. *Progress in Brain Research, 142*, 225–42, https://doi.org/10.1016/S0079-6123(03)42016-5.

Monaco, S., Kroliczak, G., Quinlan, D. J., Fattori, P., Galletti, C., Goodale, M. A., . . . Culham, J. C. (2010). Contribution of visual and proprioceptive information to the precision of reaching movements. *Experimental Brain Research, 202*(1), 15–32, https://doi.org/10.1007/s00221-009-2106-9.

Novelli, G., Papagno, C., Capitani, E., Laiacona, M., Cappa, S., & Vallar, G. (1986). Three clinical tests for the assessment of verbal long-term memory function. Norms from 320 normal subjects. *Archive of Psychology, Neurology and Psychiatry, 47*, 278–296.

Orsini, A., Grossi, D., Capitani, E., Laiacona, M., Papagno, C., & Vallar, G. (1987). Verbal and spatial immediate memory span: normative data from 1355 adults and 1112 children, *8*(6), 539–548.

Osterrieth, P. A. (1944). Le test de copie d'une figure complexe; contribution à l'étude de la perception et de la mémoire. [Test of copying a complex figure; contribution to the study of perception and memory.]. *Archives de Psychologie, 30*, 206–356.

Pélisson, D., Prablanc, C., Goodale, M. A., & Jeannerod, M. (1986). Visual control of reaching movements without vision of the limb. *Experimental Brain Research, 62*(2), 303–311, https://doi.org/10.1007/BF00238849.

Perenin, M. T., & Vighetto, A. (1988). Optic ataxia: a specific disruption in visuomotor mechanisms. I. Different aspects of the deficit in reaching for objects. *Brain : A Journal of Neurology, 111*(3), 643–674.

Pisella, L., Gréa, H., Tilikete, C., Vighetto, A., Desmurget, M., Rode, G., . . . Rossetti, Y. (2000). An "automatic pilot" for the hand in human posterior parietal cortex: Toward reinterpreting optic ataxia. *Nature Neuroscience, 3*(7), 729–736, https://doi.org/10.1038/76694.

Pisella, L., Michel, C., Gréa, H., Tilikete, C., Vighetto, A., & Rossetti, Y. (2004). Preserved prism adaptation in bilateral optic ataxia: Strategic versus adaptive reaction to prisms. *Experimental Brain Research, 156*(4), 399–408, https://doi.org/10.1007/s00221-003-1746-4.

Piserchia, V., Breveglieri, R., Hadjidimitrakis, K., Bertozzi, F., Galletti, C., & Fattori, P. (2017). Mixed body/hand reference frame for reaching in 3D space in macaque parietal area PEc. *Cerebral Cortex (New York, N.Y. : 1991), 27*, 1976–1990, https://doi.org/10.1093/cercor/bhw039.

Prablanc, C., & Martin, O. (1992). Automatic control during hand reaching at undetected two-dimensional target displacements. *Journal of Neurophysiology, 67*(2), 455–469, https://doi.org/10.1152/jn.1992.67.2.455.

Rice, N. J., Edwards, M. G., Schindler, I., Punt, T. D., McIntosh, R. D., Humphreys, G. W., . . . Milner, A. D. (2008). Delay abolishes the obstacle avoidance deficit in unilateral

optic ataxia. *Neuropsychologia, 46*(5), 1549–1557, https://doi.org/10.1016/j.neuropsychologia.2008.01.012.

Rorden, C., & Brett, M. (2000). Stereotaxic display of brain lesions. *Behavioural Neurology, 12*, 421719, https://doi.org/10.1155/2000/421719.

Rossetti, Y., Pisella, L., & Vighetto, A. (2003). Optic ataxia revisited. *Experimental Brain Research, 153*(2), 171–179, https://doi.org/10.1007/s00221-003-1590-6.

Sainburg, R. L., Lateiner, J. E., Latash, M. L., & Bagesteiro, L. B. (2003). Effects of altering initial position on movement direction and extent. *Journal of Neurophysiology, 89*(1), 401–415, https://doi.org/10.1152/jn.00243.2002.

Schaadt, A., Brandt, S., Kraft, A., & Kerkhoff, G. (2015). Holmes and Horrax (1919) revisited: Impaired binocular fusion as a cause of "flat vision" after right parietal brain damage - A case study. *Neuropsychologia, 69*, 31–38.

Schindler, I., Rice, N. J., McIntosh, R. D., Rossetti, Y., Vighetto, A., & Milner, A. D. (2004). Automatic avoidance of obstacles is a dorsal stream function: evidence from optic ataxia. *Nature Neuroscience, 7*(7), 779–784, https://doi.org/10.1038/nn1273.

Snyder, L., Batista, A., & Andersen, R. (1997). Coding of intention in the posterior parietal cortex. *Nature, 386*, 167–170.

Spinnler, H., & Tognoni, G. (1987). Standardizzazione e taratura italiana di test neuropsicologici. *Masson Italia periodici, Milano e 1987*.

Striemer, C., Locklin, J., Blangero, A., Rossetti, Y., Pisella, L., & Danckert, J. (2009). Attention for action? Examining the link between attention and visuomotor control deficits in a patient with optic ataxia. *Neuropsychologia, 47*(6), 1491–1499, https://doi.org/10.1016/j.neuropsychologia.2008.12.021.

van Beers, R. J., Sittig, A. C., & Denier van der Gon, J. J. (1998). The precision of proprioceptive position sense. *Experimental Brain Research, 122*(4), 367–77. Retrieved from http://www.ncbi.nlm.nih.gov/pubmed/9827856.

Van Pelt, S., & Medendorp, W. P. (2008). Updating target distance across eye movements in depth. *Journal of Neurophysiology, 99*, 2281–2290, https://doi.org/10.1152/jn.01281.2007.

Vindras, P., Desmurget, M., & Viviani, P. (2005). Error parsing in visuomotor pointing reveals independent processing of amplitude and direction. *Journal of Neurophysiology, 94*(2), 1212–1224, https://doi.org/10.1152/jn.01295.2004.

Zhang, C. Y., Aflalo, T., Revechkis, B., Rosario, E. R., Ouellette, D., Pouratian, N., ... Andersen, R. A. (2017). Partially mixed selectivity in human posterior parietal association cortex. *Neuron, 95*(3), 697–708.e4, https://doi.org/10.1016/j.neuron.2017.06.040.

Zimmermann, P., & Fimm, B. (1992). *Testbatterie zur Aufmerksamkeitsprufung (TAP)*. Freiburg: Psytest.

Zoccolotti, P., Pizzamiglio, L., Pittau, P., & Galati, G. (1994). *Batteria di Test per l'esame dell'Attenzione.* PSYTEST, Roma.